DOC. NO.
MR-N-287
NARF-61-41T

THE APPLICATION OF INVARIANT IMBEDDING TO SHIELDING PROBLEMS

U S A F

NUCLEAR AEROSPACE RESEARCH FACILITY

operated by

GENERAL DYNAMICS | FORT WORTH

DOC. NO.
MR-[illegible]7
NARF [illegible]-41T

DOC. NO.
MR-N-287
NARF-61-41T

USAF

NUCLEAR AEROSPACE RESEARCH FACILITY

9 MARCH 1962

THE APPLICATION OF INVARIANT IMBEDDING TO SHIELDING PROBLEMS

R. E. BEISSNER

SECTION II, TASK I, ITEM 7
OF FZM 2386

CONTRACT
AF 33(657)7201

ISSUED BY THE
ENGINEERING
DEPARTMENT

GENERAL DYNAMICS | FORT WORTH

ABSTRACT

The fundamental concepts of the theory of invariant imbedding as applied to particle transport processes are reviewed and their applications to shielding problems are discussed. Two new approximate methods for predicting the transmission of particles through slabs of material are derived from the imbedding equations. One-velocity computations of the angular distributions of particles reflected and transmitted by slabs of varying thickness and composition are presented and analyzed.

SUMMARY

Invariant imbedding is a new approach to the derivation of transport equations and results in a formulation quite different from the usual Boltzmann formulation. It yields equations for the fluxes transmitted and reflected by a body as a function of the dimensions of the body. For this reason it is particularly well suited to shielding studies in which shield thickness is considered as a parameter. This report summarizes the development of the imbedding theory and discusses shielding applications of the theory.

The imbedding and Boltzmann approaches are compared to illustrate the essential differences in the resulting equations. It is noted that, in general, the imbedding method yields initial-value rather than two-point boundary-value problems as does the Boltzmann method. The resulting computational advantages of the imbedding formulation are discussed.

The imbedding equations for the transmitted and reflected energy and angular distributions in a slab geometry are derived. Extension of the method to other geometries and multilayer configurations is discussed. Methods for applying the imbedding equations to the prediction of emergent neutron, gamma, neutron-induced gamma, and photoneutron distributions are presented. It is shown that the equations for these processes are of the

same form and, further, that they may be solved simultaneously by the same techniques used in obtaining primary neutron or gamma-ray solutions. The use of imbedding methods in shield optimization studies is discussed briefly. Methods for obtaining approximate solutions to thick-slab penetration problems are presented.

A FORTRAN Procedure, R61, coded for the IBM-7090 to solve the imbedding equations for a slab, is described. Numerical results of some R61 calculations of one-velocity, emergent angular distributions are presented. A simplified model is developed and applied in the analysis of these data to facilitate qualitative comparisons of angular distributions as a function of slab thickness, absorption probability, and angular scattering cross section. As a result of the numerical studies a method which results in further simplification of the thick-slab penetration problem is developed

It is concluded that the method of invariant imbedding is potentially a powerful tool for theoretical studies of shielding problems as well as for the generation of parametric data for shield-design studies.

TABLE OF CONTENTS

TABLE OF CONTENTS (Cont'd)

LIST OF FIGURES

I. INTRODUCTION

The development of invariant imbedding began with the work of the Russian astrophysicist, Ambarzumian, who derived an equation for the reflection of light from an infinite half space (Ref. 1). The solution was obtained by Chandrasekhar (Ref. 2). Although this work was of great theoretical importance because it constituted a new approach to transport theory, it was largely ignored by workers in neutron transport theory until a few years ago. During the past five years Bellman, Kalaba and Wing (Ref. 3) have developed a generalization of Ambarzumian's idea which includes transport equations for finite media.

Invariant imbedding is not a method for obtaining analytic or numerical solutions to the Boltzmann equation. It is a new approach to the derivation of transport equations - quite different from the usual Boltzmann approach. In fact, it is more general than particle transport theory itself. Imbedding techniques are now being applied to problems involving wave processes (Ref. 3). For our purposes, however, it may be considered as a method for obtaining new transport equations which may be easier to solve than the Boltzmann equation.

In the following sections the theory and some possible applications are presented. First, the imbedding and Boltzmann

equations are derived for a simple one-dimensional case and the differences between the two approaches are discussed. Next, the imbedding approach is applied to a more realistic problem - that of transport through a slab. Further generalizations are discussed. The last two sections deal with the application of invariant imbedding to shielding problems and certain approximations suggested by the imbedding approach.

The discussion of the theory, given in Section II, is based primarily on notes taken during a course in transport theory presented by G. M. Wing at the University of California at Los Angeles. The subject is treated in much more detail in a forthcoming book by Dr. Wing.

II. THEORY

2.1 Comparison With the Boltzmann Theory

To begin the presentation of the theory, both the Boltzmann and imbedding equations are derived for a simple (admittedly unrealistic) problem. The purpose at this point is simply to illustrate the imbedding approach and point out the differences between the imbedding and Boltzmann methods.

2.1.1 Boltzmann Method

Consider a one-dimensional rod of length x with one particle/sec incident from the right at x. No particles enter from the left. Let the position coordinate in (0,x) be z and denote the left- and right-moving fluxes by v(z) and u(z), respectively. Let the interaction cross section be σ, a constant, and let F and B be the probabilities of forward and backward scatter, respectively.

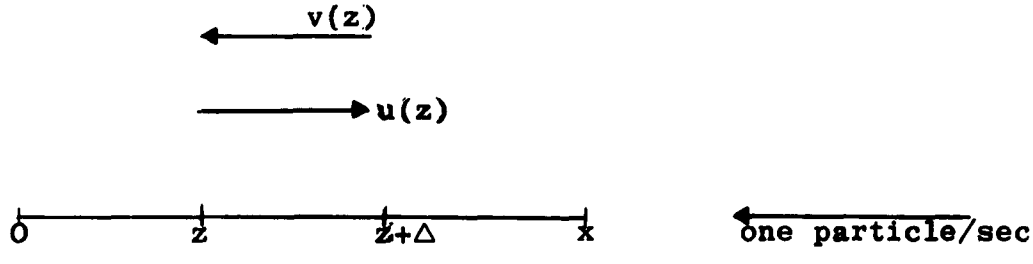

To derive the Boltzmann equations for u and v consider the fluxes at $z + \Delta$.

$$u(z+\Delta) = (1-\sigma\Delta)\, u(z) + \sigma\Delta F u(z)$$

$$+ \sigma\Delta B\, v(z) + o(\Delta)\,, \qquad (1)$$

where the terms on the right side are, to order Δ, the flux due to particles which pass from z to $z+\Delta$ having no interaction in Δ, the right-moving flux that scatters forward in Δ, and the left-moving flux scattered backward in Δ. The term $o(\Delta)$ contains all terms of order Δ^2 or higher. One might think of the right side of (1) as a Taylor's series expansion about z of the terms describing the collision processes in the increment $(z, z+\Delta)$. Taking the limit as $\Delta \longrightarrow 0$, we have

$$\lim_{\Delta \to 0} \frac{u(z+\Delta) - u(z)}{\Delta} = \lim_{\Delta \to 0} \left[-\sigma u(z) + \sigma F u(z) + \sigma B v(z) + \frac{o(\Delta)}{\Delta} \right]$$

$$\frac{du(z)}{dz} = \sigma\left[(F-1)u(z) + B v(z)\right], \qquad (2)$$

because

$$\lim_{\Delta \to 0} \frac{o(\Delta)}{\Delta} = 0\,.$$

Similarly,

$$v(z) = (1-\sigma\Delta)v(z+\Delta) + \sigma\Delta Fv(z+\Delta)$$

$$+ \sigma\Delta Bu(z) + o(\Delta) ,$$

$$-\frac{v(z+\Delta) - v(z)}{\Delta} = \sigma(F-1)v(z+\Delta)+\sigma Bu(z) + \frac{o(\Delta)}{\Delta}$$

$$-\frac{dv(z)}{dz} = \sigma \left[(F-1)v(z) + Bu(z)\right]. \qquad (3)$$

The boundary conditions are

$$v(x) = 1 \qquad (4)$$

$$u(o) = 0 . \qquad (5)$$

Equations 2 and 3 with the boundary conditions (Eqs. 4 and 5) constitute the Boltzmann formulation of the problem. Note that Equations 2 and 3 are linear and that Equations 4 and 5 are conditions at the boundaries of the transport region; thus, the arbitrary constants involved in the solution of Equations 2 and 3 are determined by the size of the rod. This means that each different size rod determines a new problem. If one wishes the reflected and transmitted fluxes u(x) and v(0), new integration constants must be determined for each rod length before these quantities can be computed. Of course, in this simple example

the integration constants are easily determined as a function of x. However, in more complex problems the determination of constants must be done numerically, thus making the determination of u(x) and v(0) quite complicated. It should be noted that the determination of the integration constants of a system of N linear, first-order equations requires the inversion of an N x N matrix for each boundary-value problem. (Systems of coupled equations of this type occur in nearly all solutions of the Boltzmann equation; e.g., Carlson S_n, spherical harmonics, and double P_ℓ.) The economics of matrix inversion on a computer is such that these equations are usually integrated numerically by some iterative scheme. This, of course, does not avoid the fact that each new configuration presents a new boundary-value problem and, thus, a new calculation. It would, therefore, be highly desirable if the transport problem could be reformulated in terms of the dimensions of the transport medium. The method of invariant imbedding provides such a formulation in many cases.

2.1.2 Invariant Imbedding Method

Consider once again the rod of transporting material with one particle/sec incident from the right. The right-moving flux at x, u(x), is the reflected flux per incident particle/sec which shall be renamed R(x). The transmitted flux per incident particle, v(0), shall be called T(x). (It is a function of the length, x,

of the rod.) The problem of predicting R(x) and T(x) is now "imbedded" in the family of problems of predicting R(x) and T(x) for various rod lengths. This is accomplished by considering the changes in R(x) and T(x) when the length of the rod is increased from x to x + Δ.

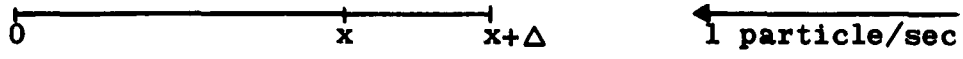

Thus,

$$\begin{aligned} R(x+\Delta) = {} & (1-\sigma\Delta)R(x)(1-\sigma\Delta) + \sigma\Delta B \\ & + \sigma\Delta F\ R(x)(1-\sigma\Delta) \\ & + (1-\sigma\Delta)R(x)\sigma\Delta F \\ & + (1-\sigma\Delta)R(x)\sigma\Delta BR(x)(1-\sigma\Delta) + o(\Delta), \end{aligned} \tag{6}$$

where $R(x+\Delta)$ is the probability of reflection by a rod of length $x+\Delta$ and R(x) is the probability for length x. The first term on the right is, to order Δ, the probability that a particle will suffer no collisions in going from $x+\Delta$ to x times the probability of reflection from the "sub-rod" of length x times the "no collision" probability for $(x, x+\Delta)$. The second term represents the back-scatter probability for the distance from $x+\Delta$ to x. The third term represents forward scatter in $(x, x+\Delta)$

followed by reflection from the sub-rod with no subsequent collisions. The fourth term represents the process in which there are no collisions in $(x, x+\Delta)$ followed by reflection by the sub-rod followed by forward scatter in $(x, x+\Delta)$. The fifth term represents no collision in $(x, x+\Delta)$, reflection by the sub-rod, scatter back into the sub-rod from $(x, x+\Delta)$, another reflection by the sub-rod and no subsequent collisions. All other processes are of order Δ^2 or higher (i.e., they involve more than one collision in Δ) and are therefore included in $o(\Delta)$. Rearrangement gives

$$\frac{R(x+\Delta) - R(x)}{\Delta} = \sigma \Big[B + FR(x) - 2R(x) + FR(x) + R(x)BR(x) \Big] + \frac{o(\Delta)}{\Delta},$$

where $o(\Delta)$ now contains the Δ^2 and Δ^3 terms from Equation 6. Letting $\Delta \longrightarrow 0$, we have

$$\frac{dR(x)}{dx} = \sigma \Big[B + 2(F-1)R(x) + R(x)BR(x) \Big], \qquad (7)$$

a first order, <u>nonlinear</u> equation for $R(x)$. The initial condition is $R(0) = 0$, which simply says that there are no particles reflected from a rod of zero length.

Similar analysis yields

$$\frac{dT(x)}{dx} = \sigma T(x)(F-1 + BR(x)),$$

with $T(0) = 1.$ (8)

At first glance it would seem that the problem has been complicated, rather than simplified, by the introduction of a nonlinear equation and, it must be admitted, nonlinear initial-value equations are typical of the imbedding approach. However, one must remember that virtually all practical problems in transport theory require the use of high-speed computers and that the numerical integration of nonlinear equations is no more difficult than the numerical integration of linear equations.

The additional fact that Equations 7 and 8 represent an initial-value rather than a two-point boundary-value problem makes numerical integration easier. Also, because these are initial-value problems, it is not necessary to carry information concerning all mesh points in the fast memory of the machine; only the last computed values are needed to perform the next step in the integration. This results in a considerable reduction in storage requirement, which is usually a major problem in transport computations. In addition to these computational advantages, the imbedding formulation provides equations with the material dimension as independent variables. Thus, the solutions to <u>one</u> problem are the

transmission and reflection values as a function of the physical dimensions of the transporting medium.

2.2 The Slab Problem

Consider the problem of energy-angular dependent transmission and reflection by slabs. To simplify the algebra the energy-angular dependence shall be represented by particle "states" with such states denoted by subscripts. Thus, particles in State i have energies which lie within some particular energy group and are traveling in a particular direction (or within a group of directions). Particles in the same energy group but with different directions of motion are considered to be in another state, say i'. The choice of a particular mode of representation (such as discrete angles, angular groups or Legendre coefficients) is not important as long as the angular dependence can be represented by discrete numbers, i.e., subscripts. Consider a slab of thickness x perturbed by the addition of a layer of thickness Δ.

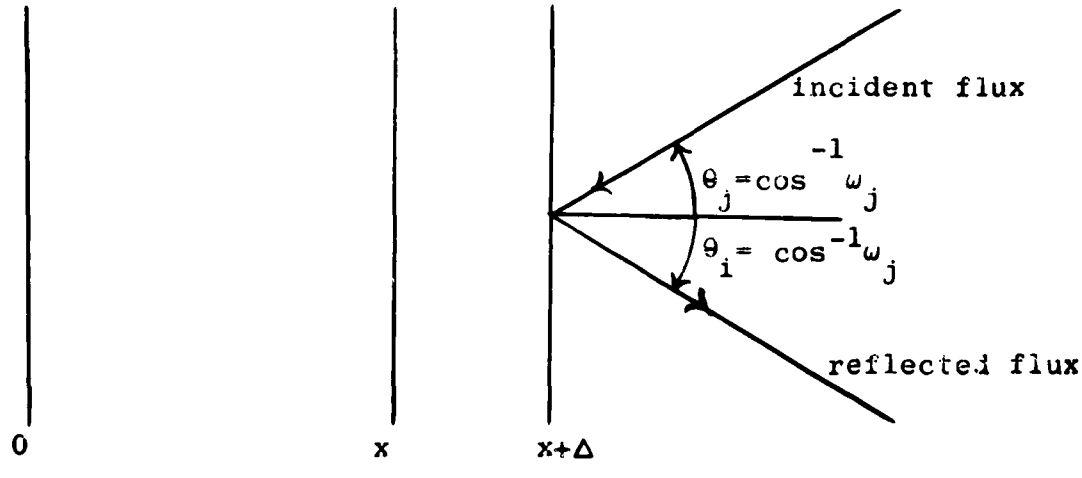

Let

σ_j = cross section for interaction of State j particles with the medium,

$\hat{F}_{ij}$ = probability that an interaction results in the transfer of particles from State j to i through a forward scatter,

$\hat{B}_{ij}$ = the corresponding probability for back-scatter, and

R_{ij} = the number of State i particles reflected through a unit area on the surface x due to one State j particle/sec incident per unit surface area.

Note that the probability that a State j particle will suffer a collision in $(x, x+\Delta)$ is $\sigma_j \Delta / \omega_j$, where ω_j is the cosine of the angle between the State j particle direction and the normal to the slab. To avoid negative values, incident angles will be measured from the inward normal and reflection angles from the outward normal. Proceeding as before, it is seen that

$$R_{ij}(x+\Delta) = \left(1 - \frac{\sigma_j}{\omega_j}\Delta\right) R_{ij}(x) \left(1 - \frac{\sigma_i}{\omega_i}\Delta\right) + \frac{\sigma_j}{\omega_j}\Delta\hat{B}_{ij}$$

$$+ \sum_k \frac{\sigma_j}{\omega_j}\Delta\hat{F}_{kj}\, R_{ik}(x) \left(1 - \frac{\sigma_i}{\omega_i}\Delta\right)$$

$$+ \sum_k \left(1 - \frac{\sigma_j}{\omega_j}\Delta\right) R_{kj} \frac{\sigma_k}{\omega_k}\Delta\hat{F}_{ik}$$

(equation continued).

$$+ \sum_k \sum_\ell \left(1 - \frac{\sigma_j}{\omega_j}\Delta\right) R_{kj}(x) \frac{\sigma_k}{\omega_k} \Delta \hat{B}_{\ell k} R_{i\ell}(x) \left(1 - \frac{\sigma_i}{\omega_i}\Delta\right)$$

$$+ o(\Delta) ,$$

where the sums on k and ℓ are over all particle states. Rearranging and taking the limit as before one obtains

$$\frac{dR_{ij}}{dx} = \frac{\sigma_j}{\omega_j} \hat{B}_{ij} - \left(\frac{\sigma_j}{\omega_j} + \frac{\sigma_i}{\omega_i}\right) R_{ij}(x)$$

$$+ \frac{\sigma_j}{\omega_j} \sum_k \hat{F}_{kj} R_{ik}(x)$$

$$+ \sum_k R_{kj}(x) \frac{\sigma_k}{\omega_k} \left[\hat{F}_{ik} + \sum_\ell \hat{B}_{\ell k} R_{i\ell}(x)\right]$$

Define the matrices

$$F = \left(\frac{\sigma_j}{\omega_j}\left[\hat{F}_{ij} - \delta_{ij}\right]\right),$$

where δ_{ij} is the Kronecker delta,

$$B = \left(\frac{\sigma_j}{\omega_j} \hat{B}_{ij}\right),$$

and $R = (R_{ij})$.

Then

$$\frac{dR(x)}{dx} = B + FR(x) + R(x)F + R(x)\,BR(x). \tag{9}$$

A similar development gives

$$\frac{dT(x)}{dx} = T(x)\,(F + BR(x)). \tag{10}$$

The initial conditions are

$$R(0) = 0 \qquad \text{(null matrix)} \tag{11}$$

$$T(0) = I \qquad \text{(identity matrix)} \tag{12}$$

which state that for a slab of zero thickness the reflected flux is zero and the transmitted flux is the same as the incident flux; i.e., $T_{ij}(0) = 0$ for $i \neq j$, and $T_{ii} = 1$. Equations 9 and 10 are a system of first-order, nonlinear equations with initial values given by Equations 11 and 12. Numerical solutions may be obtained by any of the well-known schemes for integrating such systems (Ref. 4). A FORTRAN procedure, R61, has been programmed to solve Equations 9 and 10 by the Runge-Kutta method (see Section IV). Once the Matrices R and T have been determined,

transmitted and reflected distributions may be obtained as a function of slab thickness for any incident distributions. The procedure is quite simple. Represent the incident energy-angular distribution by intensities in discrete states, S_j. Arrange these numbers in a column matrix

$$S = \begin{pmatrix} S_1 \\ S_2 \\ \vdots \\ S_N \end{pmatrix} .$$

The transmitted distribution for a slab of thickness x is the column matrix

$$\phi = \begin{pmatrix} \phi_1 \\ \phi_2 \\ \vdots \\ \phi_N \end{pmatrix} = \left(T_{ij}(x)\right) \begin{pmatrix} S_1 \\ S_2 \\ \vdots \\ S_N \end{pmatrix} .$$

Similarly, the matrix product R(x)S gives the reflected distribution. Procedure R61 computes the T and R matrices and writes these on tape for any number, up to 200, of designated thicknesses. It

is, therefore, possible to write a simple matrix multiplication procedure which would read T and R data from the R61 tape, read incident distribution data from cards or tape, and compute transmitted and reflected energy-angular distributions as a function of slab thickness.

Because of the simplicity of the slab problem it was the first to be chosen for numerical investigation. Bellman, Kalaba and Prestrud (Ref. 5) have performed reflection calculations for a one-velocity, isotropic-scatter model for slab thicknesses up to 20 mean free paths. Their computer program is similar to R61. Bellman, Kalaba and Prestrud have also obtained time-dependent results for a model with no energy or angular dependence (Ref. 6). During checkout of R61, the author obtained transmission and reflection data which are presented in Section V.

2.3 Other Geometries

Imbedding equations for cylinder and sphere problems have been derived by Bellman, Kalaba and Wing (Ref. 3). Numerical investigations have not yet been attempted; Bellman and Kalaba are planning to run some sphere problems in the near future. Wing has developed a generalized approach to the derivation of equations for other geometries (Ref. 7) and has investigated methods for transforming from the Boltzmann formulation to the imbedding equations.

Multilayered configurations offer no special difficulties. Position-dependent cross sections may be incorporated in the derivation without changing the usual procedure. The slab equations with variable cross section are the same as Equations 9 and 10 except that the F and B matrices are functions of x.

A simpler procedure for handling multilayer slabs involves changing the initial conditions. Consider a rod of two materials. Let the region from 0 to y be of one material and the region from y to the right be another material. It may be shown that

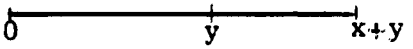

the reflection solution for the composite rod, x + y, may be obtained by solving for the reflection from the homogeneous rod (0, y) and then proceeding with the solution for the second homogeneous rod (y, x+y) subject to the new initial condition R(x=0) = R(y). A similar modification of the initial condition may be used in solving for transmission functions.

This procedure may be adapted to any multilayer configuration.

III. SHIELDING APPLICATIONS

3.1 The Combined Neutron and Gamma-Ray Problem

The application of imbedding techniques to neutron and gamma-ray penetration and reflection problems follows directly from the development outlined in the preceding sections. Application to neutron-induced gamma calculations is, perhaps, not so obvious in view of the fact that the imbedding method does not provide predictions of fluxes inside the material. It shall be shown in this section how the method can be used not only to produce secondary-gamma predictions without explicit knowledge of the internal neutron flux, but also to calculate transmission and reflection of neutrons, secondary gammas and primary gammas simultaneously.

In Section 2.2 energy-angular distributions were represented by dividing the energy-angular intervals into discrete regions or "states." Cross sections and transfer probabilities were defined for each state. As far as the mathematical development which followed is concerned, there is no reason to assume that particles in different states are even the same kind of particles. The equations are still valid if the particles in the first few states are neutrons and those in the remaining states are gamma rays. To illustrate, consider a simple two-state problem in which particles in State 1 are neutrons and those in State 2 are gamma rays. Then σ_1 and σ_2 are, respectively, neutron and

gamma-ray collision cross sections. F_{11}, B_{11}, F_{22} and B_{22} are neutron and gamma-ray forward- and back-scatter probabilities. F_{21} is the probability that a neutron collision results in a gamma-ray traveling in the precollision neutron direction. B_{21} has a similar definition, but implies a reversal of direction. F_{12} and B_{12} imply gamma-to-neutron conversion and will therefore be zero unless photoneutron reactions are considered. The extension to more than two states (to allow energy-angle considerations to be incorporated) is straightforward and results in partitioning of the F, B, R and T matrices as illustrated below.

$$\begin{pmatrix} (n \longrightarrow n) & (\gamma \longrightarrow n) \\ (n \longrightarrow \gamma) & (\gamma \longrightarrow \gamma) \end{pmatrix}$$

The sub-matrix $(n \longrightarrow n)$ contains the probabilities of transfer from one neutron state to another, $(n \longrightarrow \gamma)$ contains neutron-to-gamma probabilities, etc. Thus, the transmission matrix

$$T = \begin{pmatrix} T_n & T_{\gamma n} \\ T_{n\gamma} & T_{\gamma} \end{pmatrix}$$

contains the transmission matrices for neutrons, primary gamma rays, secondary gamma rays and photoneutrons. The source distribution, to which the transmission operator is applied is

$$S = \begin{pmatrix} S_n \\ \\ S_\gamma \end{pmatrix} ,$$

where S_n is the column matrix representing the incident neutrons and S_γ represents incident gamma rays. The result of the operation $\Phi = TS$ is a column matrix containing the transmitted neutrons and gamma rays, including secondary gamma rays and photoneutrons. It should be noted that the equations for the combined neutron gamma-ray problem are of the same form as those for single-particle transport. Thus, the existing code, R61, can be applied to the combined problem.

3.2 Shield Optimization

The imbedding method may also be helpful in shield optimization studies. The gradient-nonlinear programming method (Ref. 8) now used to arrive at an optimum shield configuration requires a knowledge of the derivative of the dose rate (ideally the total, neutron plus gamma, dose rate) with respect to shield weight or thickness. This is presently accomplished by solving shield transmission problems for several shield thicknesses (neutron,

gamma and secondary-gamma predictions require separate treatment), and then curve-fitting and differentiating the results. An imbedding formulation of the same problem would yield a differential equation for the transmission function for each segment of the shield. These segments might be considered sections of a sphere, in which case the imbedding equations already exist if one is willing to consider each segment independent of all others. (This assumption is made in current shield-penetration procedures.) The imbedding equations give the flux, or dose-rate, derivatives with respect to thickness explicitly in terms of the transmission and reflection functions. Thus, the entire optimization procedure, with the exception of the air-transfer operation, may be reformulated in terms of transmission and reflection matrices. As noted in the preceding section, these matrices may include all processes, including secondary-gamma production, and may be obtained for a range of shield thicknesses in a single problem. Also, note that multilayer configurations are easily handled as long as thickness variations are performed with the outer layer only.

3.3 Approximations for a Slab

Note that as the thickness of a slab increases the reflection matrix approaches a constant matrix, namely, the reflection matrix for an infinite half space, R_A. Thus, for x large enough, the transmission matrix satisfies

$$\frac{dT(x)}{dx} = T(x)(F + BR_A).$$

The solution is

$$T(x) = e^{(F+BR_A)x},$$

where the well-known matrix exponential is defined by

$$e^{(A)x} = I + Ax + A^2\frac{x^2}{2!} + A^3\frac{x^3}{3!} + \ldots .$$

The constant matrix R_A is the solution to Ambarzumian's problem and may be obtained by Chandrasekhar's method or by numerically integrating the imbedding equation until sufficiently small changes in R(x) are noted at neighboring points. The matrix exponential may be computed either from the definition, from Sylvester's theorem, or by diagonalization of the matrix $(F + BR_A)$.

The temptation to approximate T(x) by a matrix exponential leads to another approximation. Note that the term BR(x) represents a double reflection because B is the back-scatter matrix and R is the reflection matrix. If scattering is predominantly forward, one may wish to ignore multiple reflections of the type illustrated

below and

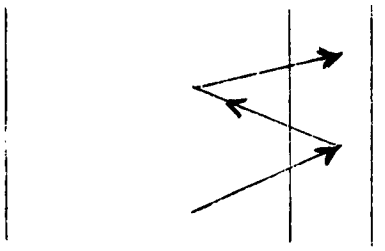

represented by the term BR. It is not necessary to assume that either B or R is negligible, only that the product BR is negligible compared to the forward-scatter matrix F. Then the transmission is approximated by

$$T(x) = e^{Fx}$$

and the reflection by the solution of

$$\frac{dR(x)}{dx} = B + FR + RF.$$

In the reflection equation the term RBR has been neglected.

IV. NUMERICAL STUDIES

A series of one-velocity slab penetration and reflection computations were performed that will illustrate the application of the imbedding method to shielding studies. A brief discussion of the FORTRAN Procedure R61 is given below, followed by a detailed discussion of the computations. Some of the computed data are presented along with an analysis based upon a simplified model for describing angular distributions.

4.1 FORTRAN Procedure R61

A FORTRAN Procedure, R61, was coded for the IBM-704 to investigate the transmission and reflection matrix equations. The code is based on the Runge-Kutta method (Ref. 4) and includes a check of the results after each step in the integration. A description of some of the features of the procedure follows.

In general, the numerical integration of an initial-value problem begins with a knowledge of the initial value of the dependent variable, $f(x)$, and its derivatives, and proceeds, through a series of finite steps in the independent variable, to predict the value of the dependent variable at the end point of each step. The Runge-Kutta method provides a formula for performing this stepping operation in terms of the function and its first derivative at the last mesh point considered. That is, the procedure

for computing the number $f(x+\Delta)$ in terms of $f(x)$ and $\left(\frac{df}{dx}\right)_x$ is given by the Runge-Kutta formula.

The accuracy of the computation depends, of course, on the size of the step Δ and the behavior of the function $f(x)$ in the interval $(x, x+\Delta)$. An estimate of the error involved in the computation may be obtained by first computing $f(x+\Delta)$ using the full step Δ, then recomputing $f(x+\Delta)$ by taking two successive steps of width $\Delta/2$. The error in the second (more accurate) estimate of $f(x+\Delta)$ is approximately one-fifteenth the difference between the first and second computations of $f(x+\Delta)$ (Ref. 4). This procedure is used in R61 to estimate the error. If the error in the prediction of $f(x+\Delta)$ is larger than some preassigned fraction of $f(x+\Delta)$ the entire process is repeated with Δ replaced by $\Delta/2$. This iterative process is repeated until either the error is small enough or until a preassigned maximum number of iterations have been attempted; in the latter case, the problem is terminated. The computer time required for this checking procedure is significant and hence undesirable in a production code. It was incorporated in R61 to provide a means of studying the effect of step size. Some of the results of these studies are given in the next section.

Because the Runge-Kutta method requires the function and its derivative at the last mesh point only, it was possible to save space in the fast memory of the machine by printing, writing on tape, or erasing data not pertaining to the last mesh point. This reduced storage requirement allows consideration of more energy or angular groups than would ordinarily be possible.

The forward- and back-scatter matrices, $[F_{ij}]$ and $[B_{ij}]$ (Sec. 2.2), are computed in the program from the formulas

$$-[F_{ij}] = \left[\frac{\sigma_g}{\omega_{j'}} \delta_{i'j'} \delta_{gg'} - \frac{Q_{i'}Q_{j'}}{\omega_{j'}} \sum_{\ell=0}^{L} \frac{2\ell+1}{2} A^{\ell}_{gg'} P_\ell(\omega_{i'})P_\ell(\omega_{j'})\right],$$

$$[B_{ij}] = \left[\frac{Q_{i'}Q_{j'}}{\omega_{j'}} \sum_{\ell=0}^{L} \frac{2\ell+1}{2} A^{\ell}_{gg'}(-1)^{\ell} P_\ell(\omega_{i'})P_\ell(\omega_{j'})\right],$$

$i = MW\,(g-1) + i'$,

$j = MW\,(g'-1) + j'$,

where

σ_g is the total cross section for energy group g,

$\omega_{i'}$ is the cosine of the angle,

δ_{ij} is the Kronecker delta,

$Q_{i'}$ is the weight factor associated with angle i' arising from the representation of an integral over angle by a finite sum,

$A^{\ell}_{gg'}$ is the ℓth Legendre coefficient of the angular group transfer cross section for scattering from energy group g' to g (Ref. 9),

$P_{\ell}(\omega)$ is the ℓth Legendre polynomial, and

MW is the number of discrete ordinates considered in the angle quadrature.

The weights, Q_i, occur when the imbedding equations are derived with continuous angle dependence and then reduced to the discrete form indicated in Section 2.2 by a suitable quadrature formula. In this case, the first term on the right side of Equation 9 (Sec. 2.2) is not the B matrix defined above, but another matrix, B^*, defined by

$$\left[B^*_{ij}\right] = \left[\frac{1}{\omega_j} \sum_{\ell=0}^{L} \frac{2\ell + 1}{2} A^{\ell}_{gg'} (-1)^{\ell} P_{\ell}(\omega_i) P_{\ell}(\omega_j)\right].$$

The derivation of these relations from the definition

$$\sigma_{gg'}(\omega) = \sum_{\ell} \frac{2\ell + 1}{4\pi} A^{\ell}_{gg'} P_{\ell}(\omega)$$

is straightforward. Here $\sigma_{gg'}(\omega)$ is the cross section for scattering from group g' to g via the scattering angle $\cos^{-1}\omega$. The coefficients, $A^{\ell}_{gg'}$, which are input for R61, are computed in another program, C54 (Ref. 9).

The program output consists of the transmission and reflection matrices, printed and written on tape, at preselected slab thicknesses. The printed output is a square array of numbers, each column (j) of which represents a particular initial state and each row (i) of which corresponds to a particular final state. Thus, the number N_{ij}, located in the array according to conventional matrix notation, is the probability of reflection or transmission for initial State j and final State i. The States i and j are related to the initial and final energies and angles by the relations given earlier.

4.2 Angular Distribution Computations

The calculations presented in Section 4.3 are based on a five-point Legendre-Gauss approximation to the angle integration. Thus, the Q_i are the Legendre-Gauss weights and the ω_i are the corresponding arguments for the interval (0, 1). Because the problems involve no energy degradation, the coefficients $A^{\ell}_{gg'}$ reduce to the Legendre coefficients in the expansion of the angular cross section. For simplicity the total cross section was set equal to unity which, in effect, is the same as measuring all distances in mean free paths. The spatial mesh points were so chosen that the interval widths become larger as the slab thickness increases. This was intended to take advantage of the fact that the most rapid changes in both the transmission and reflection functions occur for small thicknesses. As mentioned

earlier (Sec. 4.1), R61 will reduce the width of an interval if the error involved in that step is larger than some pre-assigned fraction of the function. For the problems presented here a maximum error of 1% per step was allowed. In one of the problems the intervals were chosen as large as one mean free path near the end of the integration to allow the program to determine, within a factor of 2, the optimum interval for that thickness (near 10 mean free paths). Three interval divisions occurred which left the interval width at 1/8 mean free path. Because the reflection function was changing very little at that thickness, the interval requirement is believed to have been determined by the transmission function only. This indicates that if reflection data are all that are desired, the omission of the transmission calculation could reduce the machine time by more than a factor of 2 through the use of larger mesh-point intervals for large thicknesses.

To begin the integration, step widths of about 0.010 mean free path were necessary for thicknesses up to about 0.1 mean free path. Beyond that point it was possible to increase the intervals gradually up to about 0.10 mean free path. Apparently, when both transmission and reflection calculations are to be performed, it would be more economical to use a constant interval width after the first few steps and thus avoid the checking

procedure after each step. The proper constant interval could be determined by using the interval division process out to some point, say 1 mean free path, and holding the interval constant from that point on. Elimination of the check after each step should cut computing time requirements to 2/3 that of R61.

The choice of the Runge-Kutta method for the integration was rather arbitrary. It may be possible to reduce the computer time by using other standard techniques or by developing special quadrature formulas. The asymptotic behavior of the reflection and transmission matrices might be used as a guide in developing such procedures.

Computer times for the three R61 problems presented in the next section averaged 10 minutes each. The number of mesh points required per problem varied from about 200 to 250.

4.3 Analysis of Data

The numerical results presented in this section were obtained during checkout of R61. The problems were chosen to provide data for an analysis of the angular distribution of particles reflected and transmitted by slabs. The analysis was restricted to one-velocity problems and simple angle-dependent cross sections. While the generation of data for practical problems is possible with R61, it is expected that a full-scale attack at this time would yield only a multitude of numbers, overwhelmingly complicated by energy-angle

relationships, uncertainties in slowing-down approximations, and the usual numerical difficulties encountered in manipulating large systems of equations. It was expected that the study of simple problems would lead to a better understanding of the computational and physical processes involved and, thus, to more efficient methods for realistic problems.

The analysis which follows will therefore be restricted to qualitative discussions of the effects of angular cross section, absorption, and slab thickness on emergent angular distributions. These discussions will be based on certain considerations of the collision density within the slab.

4.3.1 Method of Analysis

The integral form of the one-velocity Boltzmann transport equation for a slab is

$$f(z,\omega) = \int_{S=0}^{S_{max}} e^{-\sigma_T S} \int_{\vec{\Omega}'} f(z',\omega')\, \sigma(\vec{\Omega}' \rightarrow \vec{\Omega})\, d\vec{\Omega}'\, dS \,,$$

where $f(z,\omega)$ is the angular flux at z in the direction $\vec{\Omega}$ and S is the slant distance illustrated on the following page.

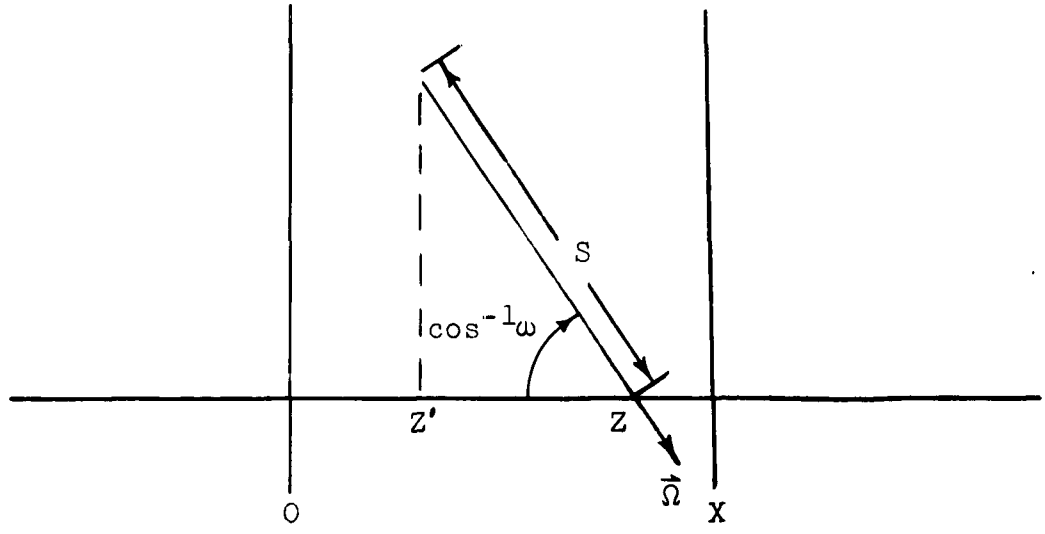

The substitution $S = \frac{z-z'}{\omega}$ gives

$$f(z,\omega) = \frac{1}{\omega}\int_0^z e^{-\sigma_T \frac{z-z'}{\omega}} \int_{\vec{\Pi}'} f(z',\omega')\sigma(\vec{\Pi}'\rightarrow\vec{\Pi})d\vec{\Pi}'dz'$$

for $\omega > 0$. The equation for the number of particles/sec passing through a unit area parallel to the slab faces is obtained by multiplying by ω:

$$\omega f(z,\omega) = \int_0^z e^{-\sigma_T \frac{z-z'}{\omega}} \int_{\vec{\Pi}'} f(z',\omega')\sigma(\vec{\Pi}'\rightarrow\vec{\Pi})d\vec{\Pi}'dz' \ .$$

The mean value theorem gives

$$\omega f(z,\omega) = e^{-\sigma_T \frac{z-\xi}{\omega}} \int_0^z \int_{\vec{\Omega}'} f(z',\omega')\sigma(\vec{\Omega}' \longrightarrow \vec{\Omega}) d\vec{\Omega}' \, dz' \ ,$$

where $\xi (0 \leq \xi \leq z)$ is some average attenuation distance determined by the collision density, $\int_{\vec{\Omega}} f(z',\omega')\sigma(\vec{\Omega} \longrightarrow \vec{\Omega}')d\vec{\Omega}'$, on the conical surface defined by ω (see sketch).

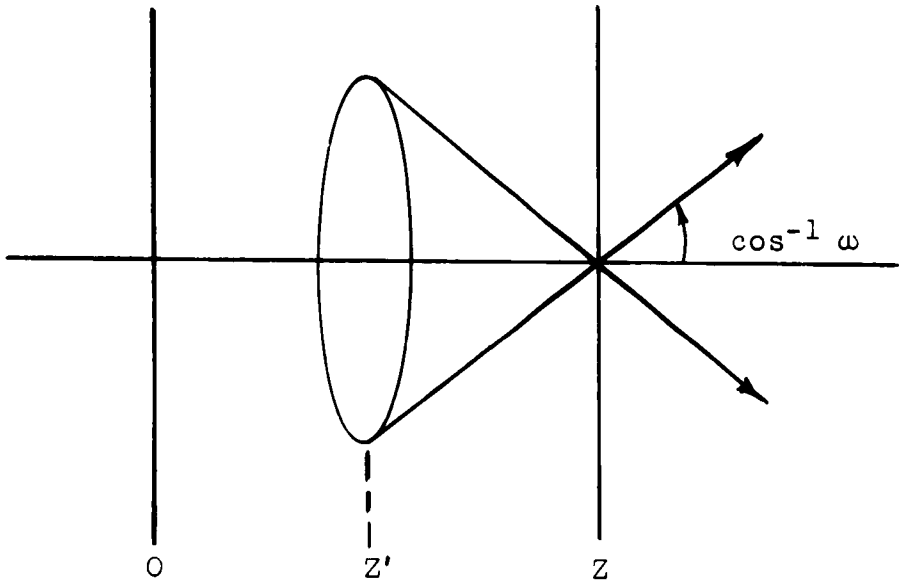

If the flux within the slab has a large maximum near $z' = 0$, the average attenuation length will be close to z. On the other hand, if the flux is rather flat as a function of z' the average length will be less than z. In the first case, the transmitted angular distribution at z will tend to be more strongly peaked

toward the slab normal than in the second case. This can be seen by examining the factor $e^{-\sigma_T \frac{z-\xi}{\omega}}$ as a function of ω for $\xi = 0$ and $\xi > 0$. Of course, the angular dependence of the collision density also affects the resulting distribution, but in a more complicated manner. This effect will be considered briefly in the numerical study to be presented later.

Reflected angular distributions may be studied by considering the equation for $\omega < 0$ (see sketch):

$$|\omega| f(z, \omega) = e^{-\sigma_T \frac{\xi - z}{|\omega|}} \int_z^x \int_{\vec{\Omega}'} f(z', \omega') \sigma(\vec{\Omega}' \longrightarrow \vec{\Omega}) d\vec{\Omega}' \, dz' ,$$

where

$$z \leq \xi \leq x.$$

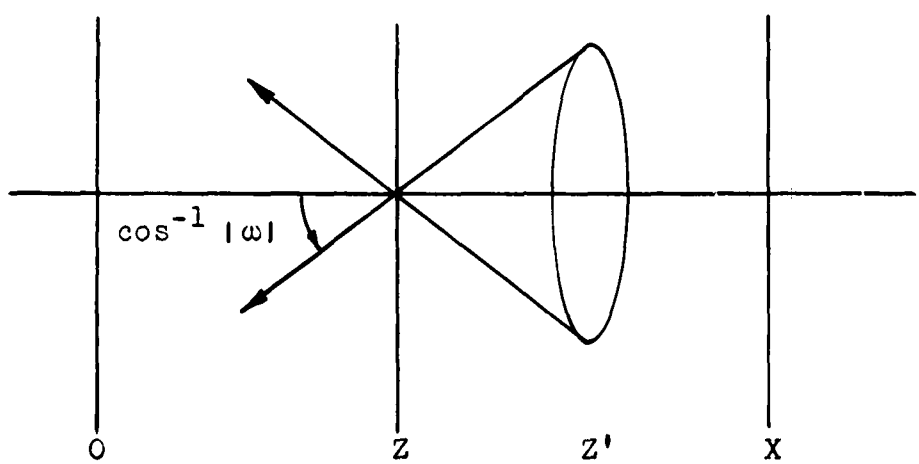

In this case a rapidly decaying spatial distribution implies $\xi \simeq z$ which, in turn, implies that the attenuation term is of little significance except for small ω. It would then be expected that the angular collision density would be the dominant factor in determining the shape of the reflected distribution. If, however, the flux distribution did not depend so strongly on z', the increased importance of the attenuation term would be expected to cause some peaking of the reflected distribution toward the slab normal.

Although the preceding arguments were applied to internal angular fluxes, they are also applicable to surface distributions and may, therefore, be used to analyze reflected and transmitted distributions as a function of slab thickness. If the internal flux distribution is strongly peaked at one surface of the slab, an increase in slab thicknesses should have little effect on the shape of either the reflected or transmitted angular distribution except, perhaps, for some increased peaking in the transmitted distribution. Of course, a large variation in the internal flux from one surface to the other implies a rather thick slab to begin with. If there is little variation in the flux throughout the slab, as would be the case in a thin slab, an increase in thickness would be expected to produce more peaking in both the reflected and transmitted distributions.

To determine the significance of the various effects just described, it was necessary to perform calculations of reflected and transmitted fluxes as a function of slab thickness, absorption and angular scattering cross section. Another parameter of some interest is the incident-particle direction as it influences the internal flux distribution within the first few mean free paths from the entrance boundary. Information concerning the effects of slab thickness and incident direction is obtained from a single problem when the imbedding method is used because they are the independent variables in the imbedding formulation. To study the effects of absorption and angular cross section it was necessary to run additional problems. Three cases were considered: 1) isotropic scatter with the absorption cross section equal to 1% of the total cross section; 2) isotropic scatter with the absorption cross section equal to one-half the total cross section; and 3) anisotropic scatter with no absorption. The anisotropic cross section used was that for hydrogen: $\sigma(\omega) = \omega/\pi$ for $\omega > 0$, $\sigma(\omega) = 0$ for $\omega < 0$, where ω is the angle of scatter. The data presented in this section are in terms of particles/sec passing through a unit area on the slab surface due to one particle/sec entering a unit area on the surface. All distances are measured in mean free paths. Note that the source strength is given in terms of particles passing through a unit area on the surface; the data should therefore be multiplied

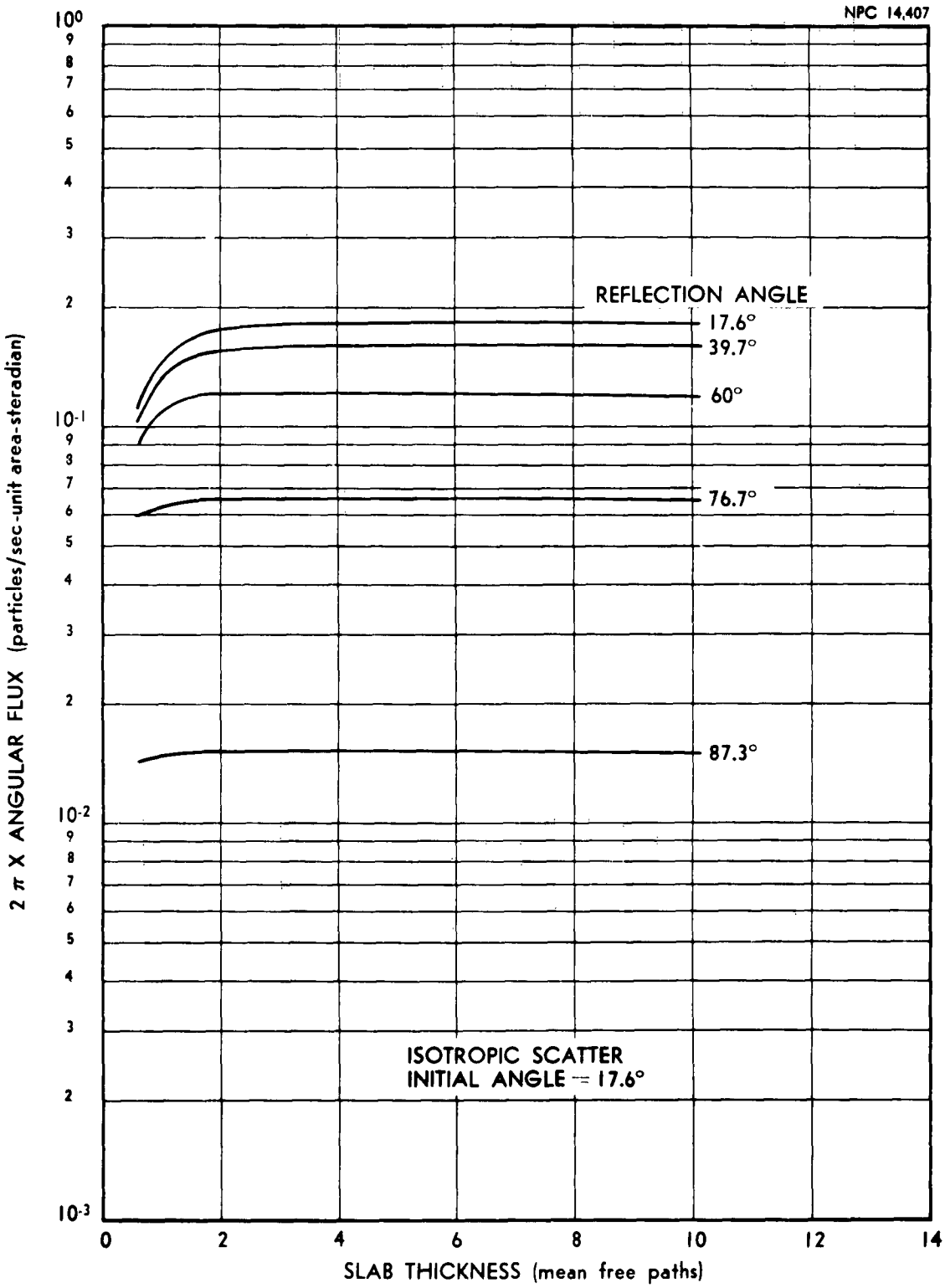

FIGURE 1. REFLECTED ANGULAR FLUX AS A FUNCTION OF SLAB THICKNESS: ABSORPTION PROBABILITY = 0.5

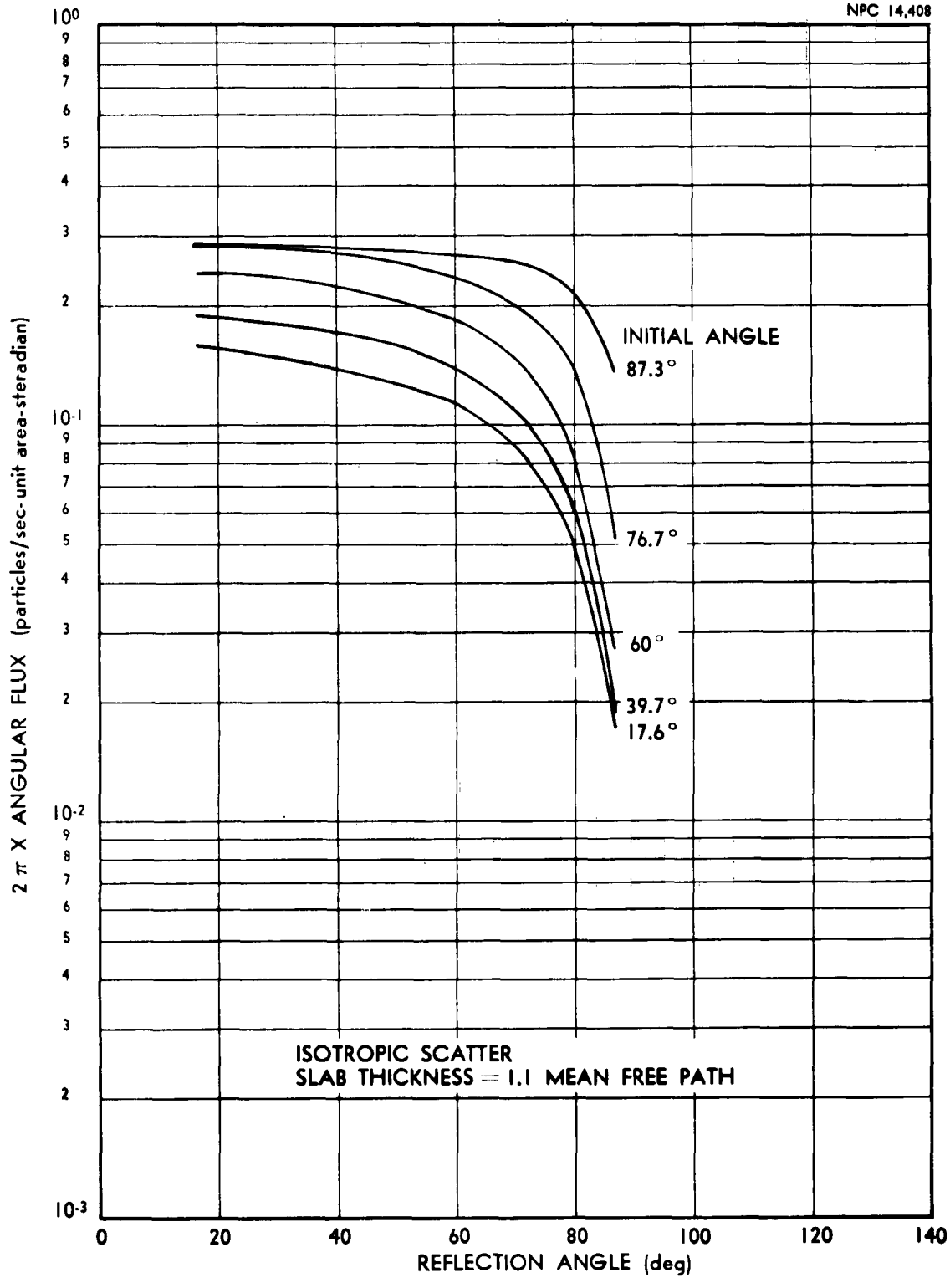

FIGURE 2A. REFLECTED ANGULAR FLUX AS A FUNCTION OF REFLECTION ANGLE: ABSORPTION PROBABILITY = 0.5

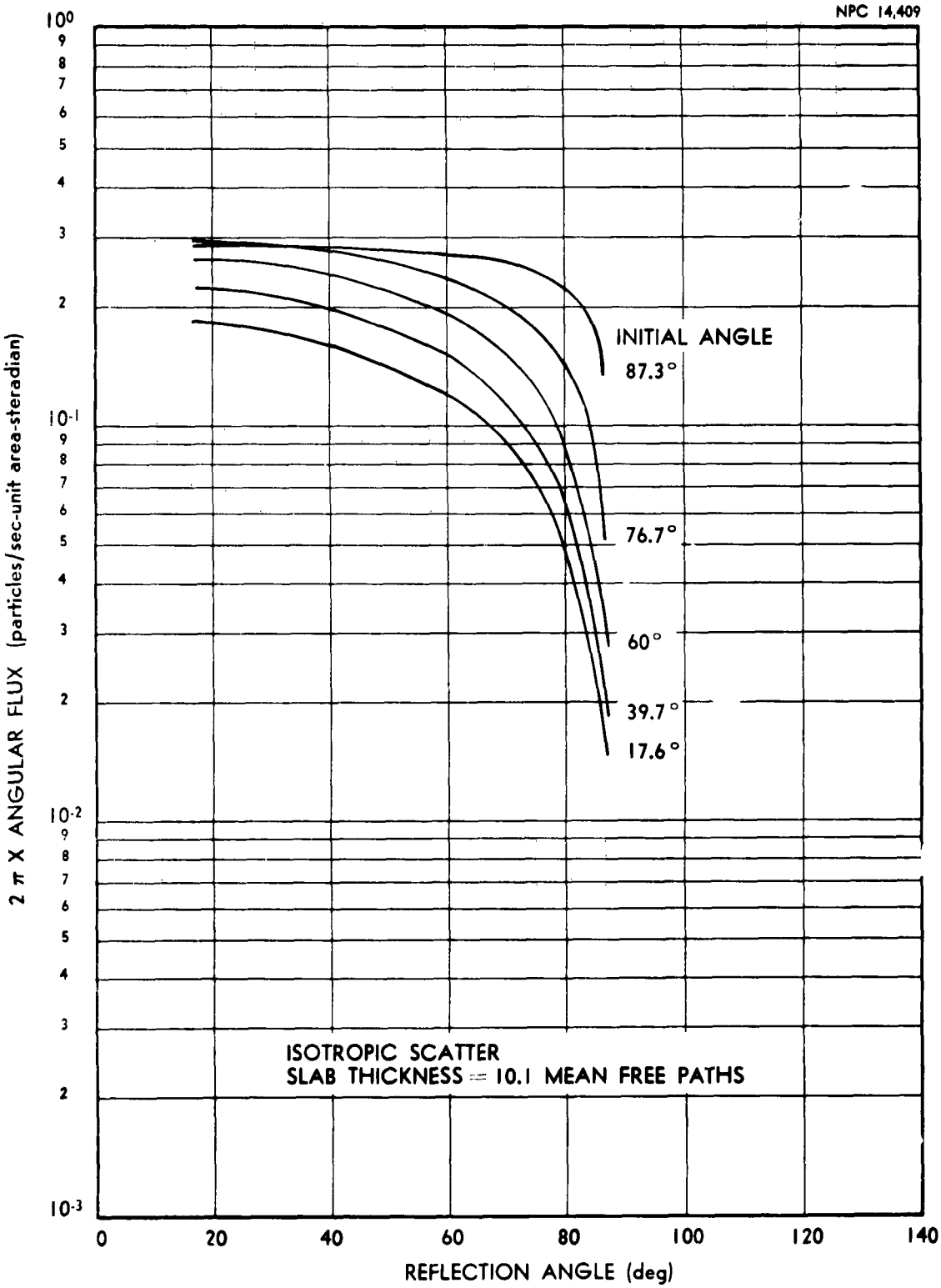

FIGURE 2B. REFLECTED ANGULAR FLUX AS A FUNCTION OF REFLECTION ANGLE: ABSORPTION PROBABILITY = 0.5

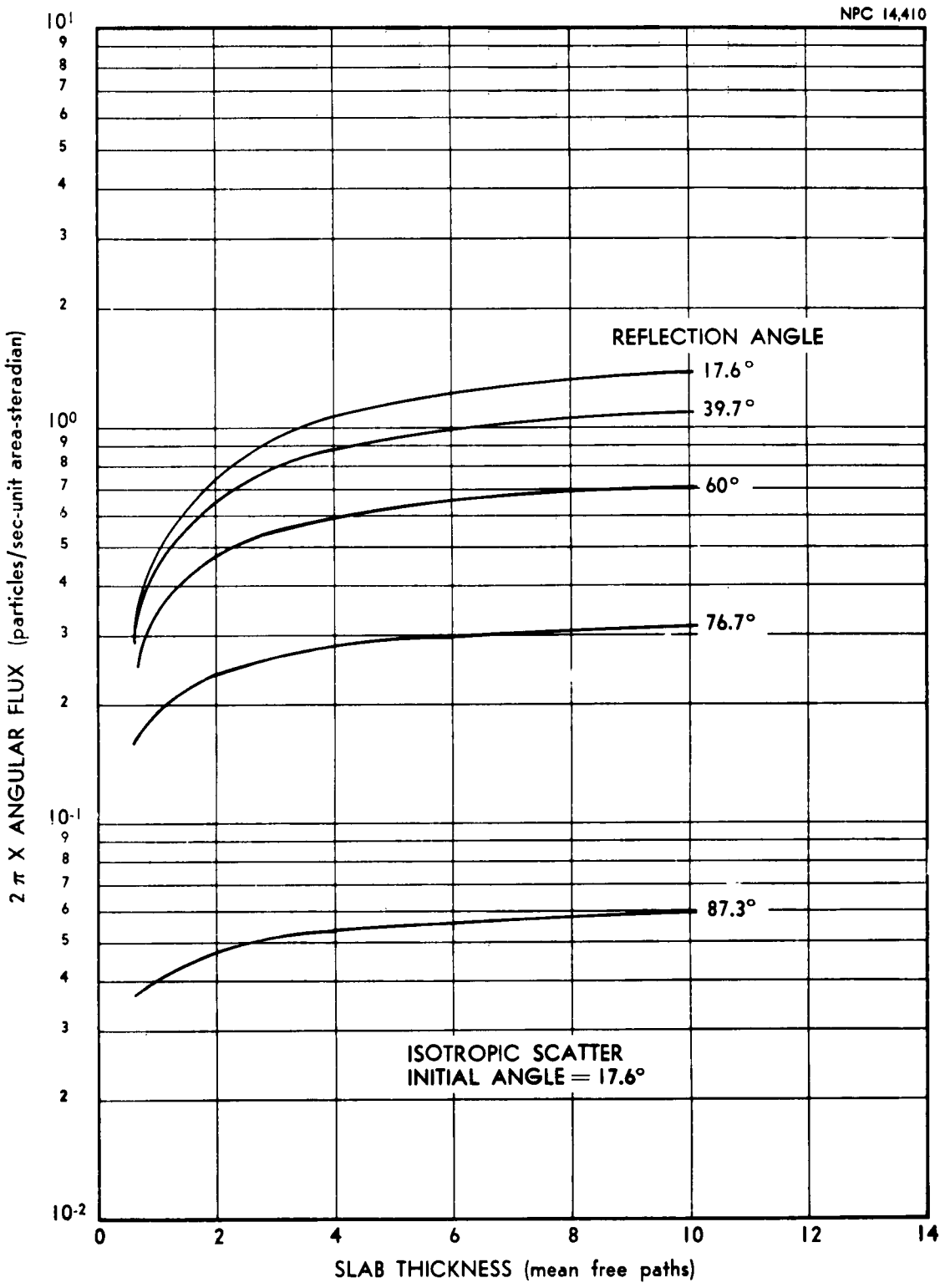

FIGURE 3. REFLECTED ANGULAR FLUX AS A FUNCTION OF SLAB THICKNESS: ABSORPTION PROBABILITY = 0.01

by the cosine of the incident angle to convert to a source of one particle/sec per unit area normal to the particle direction.

4.3.2 Reflection Calculations

Figures 1, 2A, and 2B show the reflected angular flux for isotropic scattering with the absorption cross section equal to one-half the total cross section. The first figure shows that for slab thicknesses greater than about 3 mean free paths the reflection is essentially constant. For other incident angles (not shown) the behavior is similar. Figures 2A and 2B show that the reflected angular distributions for 1.1- and 10.1-mean-free-path slabs are about the same. These distributions are rather flat, especially as the angle of incidence approaches 90°. Also, close comparison of Figures 2A and 2B shows a slight flattening of the distributions as the slab size is decreased, all of which points to the fact that a relatively high density of collision points near the entrance surface results in a flatter reflected angular distribution than a more uniform distribution of collision points. One would therefore expect that a decrease in absorption cross section, which results in less attenuation and thus a more uniform collision density, would result in more peaked reflected distributions. This effect is illustrated in Figures 3 and 4A, B, and C where the absorption is 1/100 of the total cross section. In this case the reflected distributions have not reached equilibrium even at 10 mean free paths (Fig. 3),

which indicates a much more uniform collision density in the slab than was the case with a higher absorption probability. As expected, Figures 4A and 4B show the reflected angular distributions to be more peaked toward the slab normal for the weak absorber than for the strong absorber (Figs. 2A and 2B). Figure 4C shows the effect of slab size on the reflected distribution for a 17.6° incident angle. This effect is more pronounced for the weak absorber than for the strong absorber (not shown). As the slab size is increased the reflected distribution increases over the entire range of angles but more rapidly at small angles. The result is that the angular distribution becomes more peaked as the slab size increases.

The effect of anisotropic scatter is illustrated in Figure 5. Because the scattering cross section used was peaked in the forward direction, it was expected that the collision density within the slab was extremely flat for near-normal incidence, thus giving the peaked reflected distributions. For grazing incidence, however, the forward-peaked cross section tends to concentrate the collision density near the entrance surface, thus giving extremely flat reflected distributions. In fact, in the extreme case of 87.3° incidence, the reflected distribution resembles the angular cross section because much of the reflection is due to singly scattered particles.

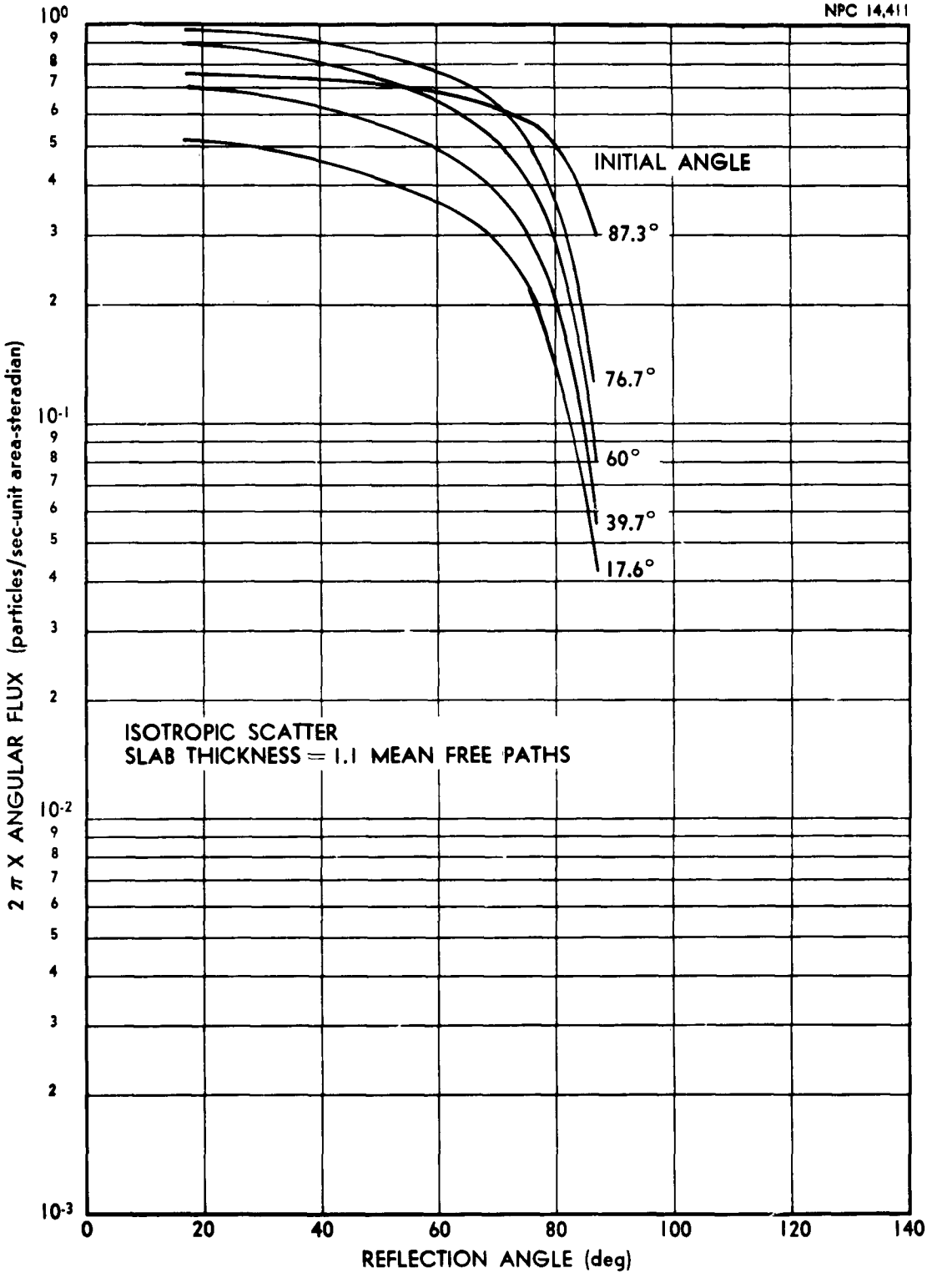

FIGURE 4A. REFLECTED ANGULAR FLUX AS A FUNCTION OF REFLECTION ANGLE: ABSORPTION PROBABILITY = 0.01

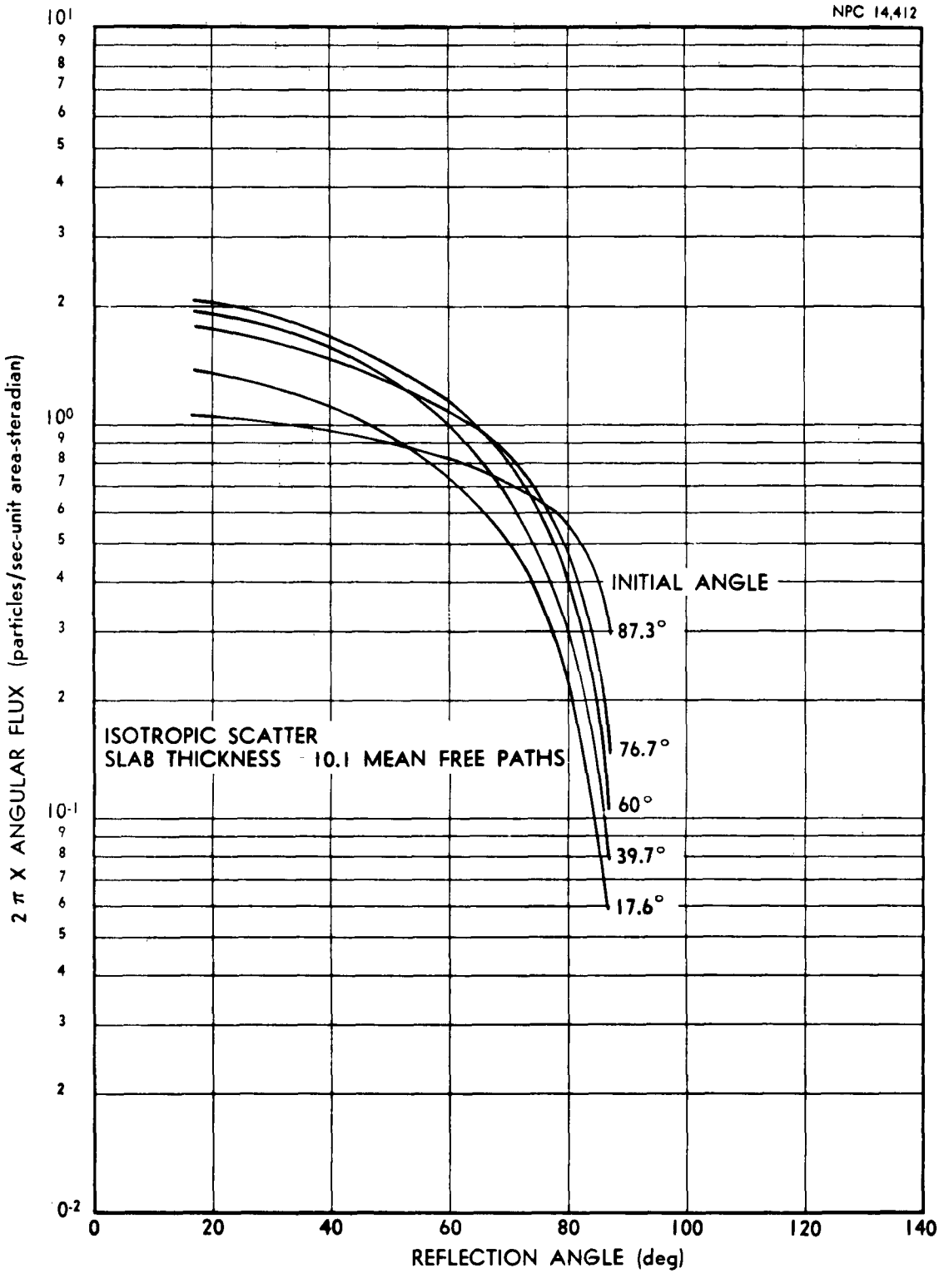

FIGURE 4B. REFLECTED ANGULAR FLUX AS A FUNCTION OF REFLECTION ANGLE: ABSORPTION PROBABILITY = 0.01

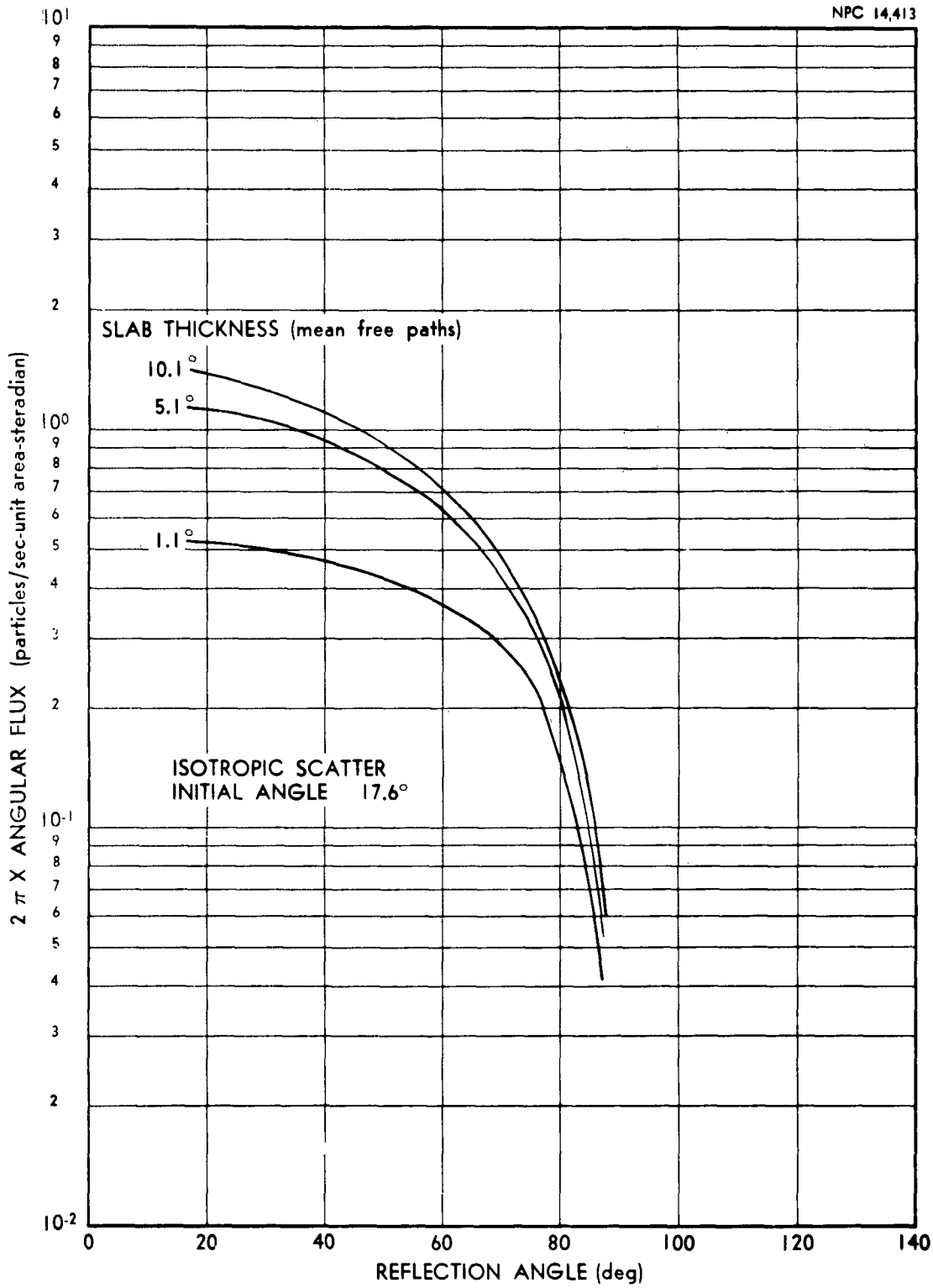

FIGURE 4C. REFLECTED ANGULAR FLUX AS A FUNCTION OF REFLECTION ANGLE: ABSORPTION PROBABILITY = 0.01

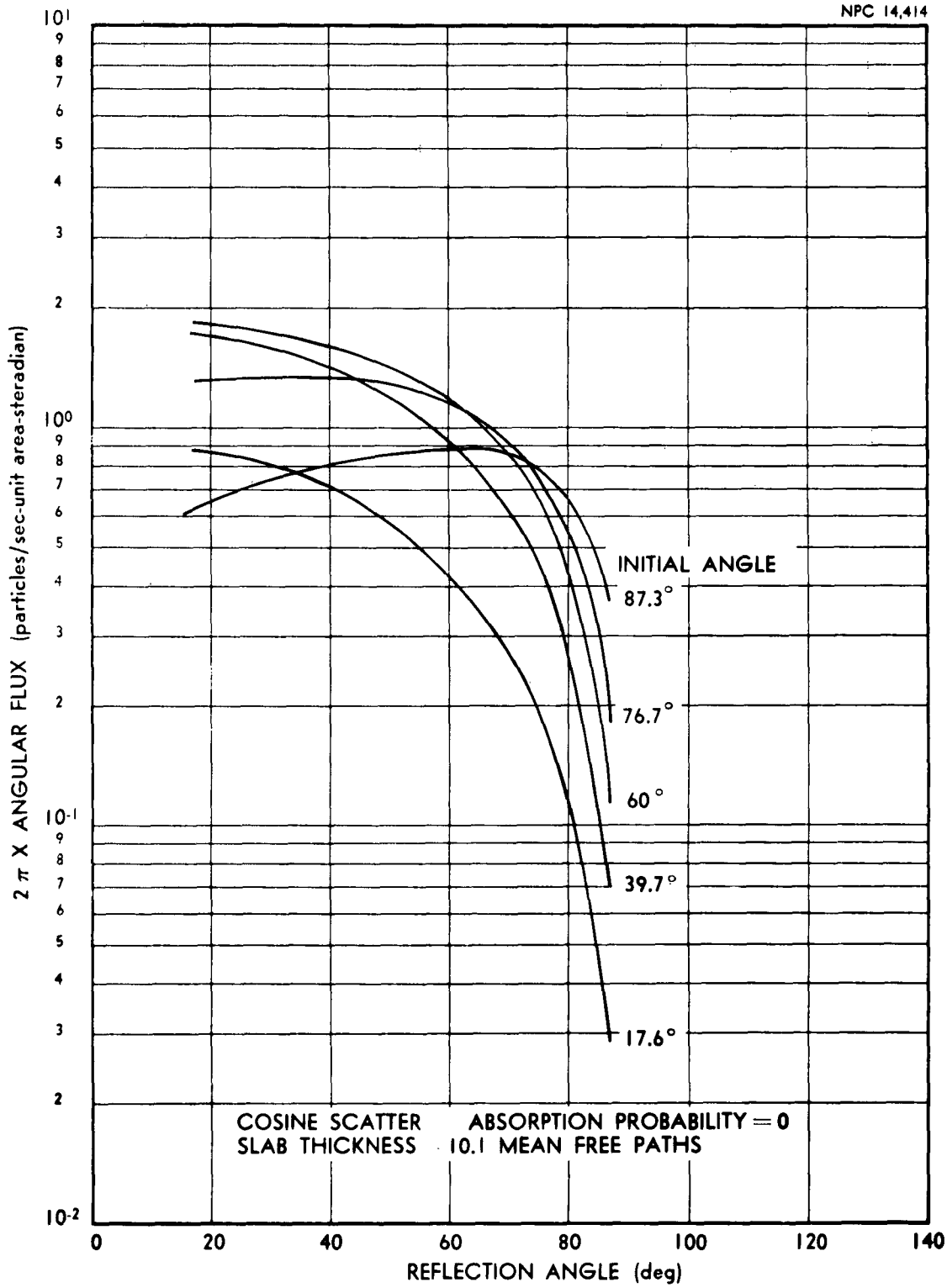

FIGURE 5. REFLECTED ANGULAR FLUX AS A FUNCTION OF REFLECTION ANGLE: ANISOTROPIC SCATTER

4.3.3 Transmission Calculations

For the transmission calculations shown in Figures 6 and 7 it was assumed that scattering was isotropic and that the absorption cross section was one-half the total cross section. As the slab thickness increases, the transmitted distribution for thick slabs decays with an almost constant relaxation length - as illustrated in Figure 6. For other incident angles (not shown), the asymptotic relaxation length is the same. However, cross plots of the angular flux, such as Figure 7, show that there is still some tendency for the angular distribution to peak in the initial direction even at 5.1 mean free paths. This is probably because the high absorption cross section prevents numerous scattering collisions which would tend to flatten this peaking. That is, the particles which are transmitted have suffered very few, if any, collisions.

The transmitted angular distributions for other incident angles are similar to those shown in Figure 7. They are generally quite peaked toward the slab normal. This is explained by the fact that the collision density, for a strong absorber, is much greater near the entrance surface and thus, as mentioned earlier, the transmitted distribution is determined largely by the attenuation suffered along the slant paths from the high-collision-density region to the exit point. When the absorption cross section is decreased the collision density inside the slab

is flattened, resulting in a longer asymptotic relaxation length (Fig. 8) and flatter angular distributions (Fig. 9). The absorption cross section used in the calculations shown in Figures 8 and 9 was 1% of the total cross section. The introduction of a forward-peaked scattering cross section lengthens the relaxation length still more (Fig. 10) and causes a very slight flattening of the transmitted angular flux (Fig. 11).

The most significant result, as far as shielding applications are concerned, is the asymptotic behavior of the transmission function. In all cases considered here, the shape of the transmitted angular distributions approached equilibrium and the magnitude of these distributions began to decay exponentially with a relaxation length characteristic of the material. These results and their obvious applications to shielding problems prompted further study of the thick-slab approximations discussed in Section 3.3. In these approximations the transmission function is the matrix exponential

$$T(x) = e^{Cx},$$

where C is a constant matrix. According to Sylvester's Theorem,

$$T(x) = \sum_{r=1}^{N} e^{\lambda_r x} z_r,$$

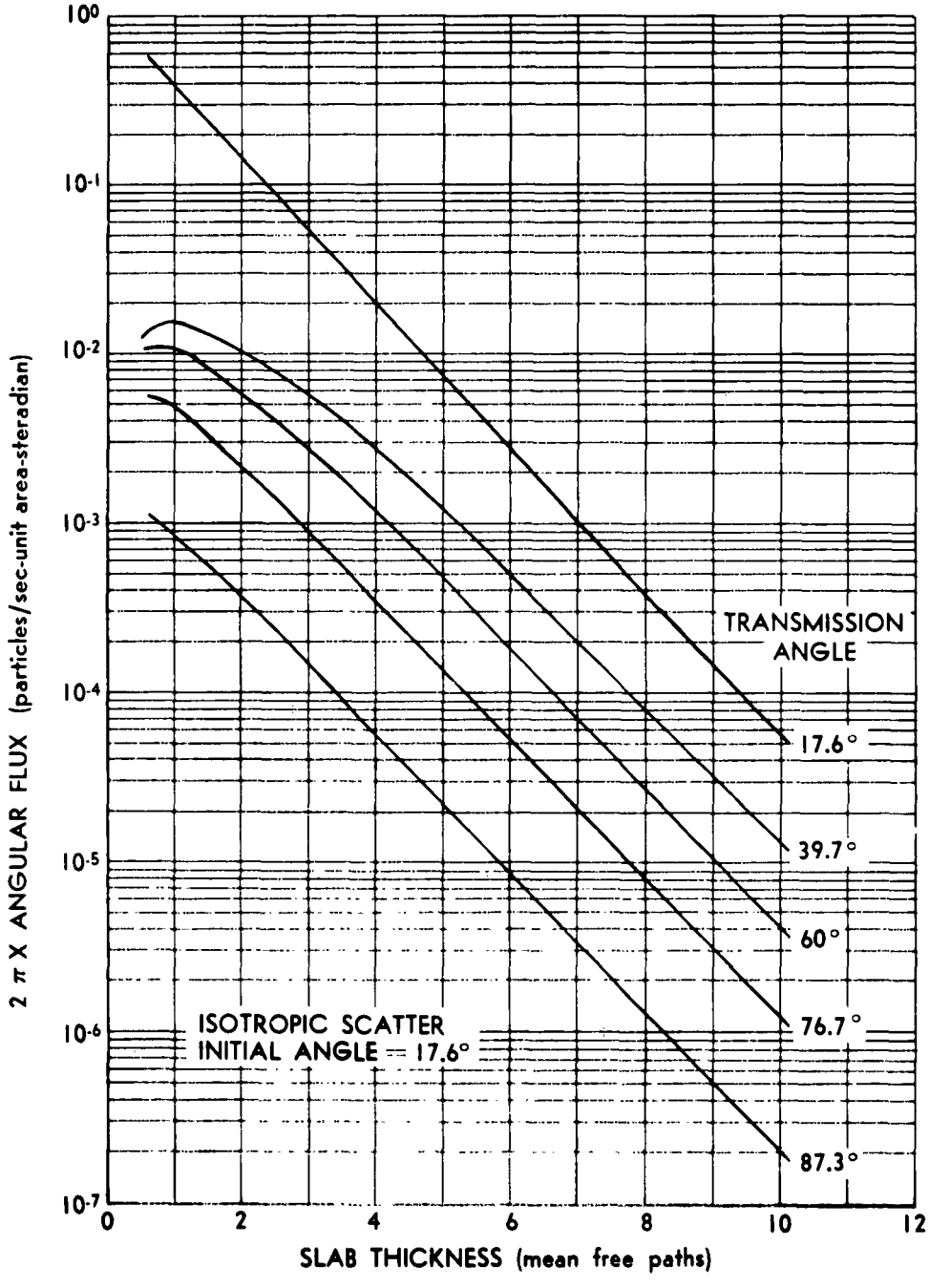

FIGURE 6. TRANSMITTED ANGULAR FLUX AS A FUNCTION OF SLAB THICKNESS: ABSORPTION PROBABILITY = 0.5

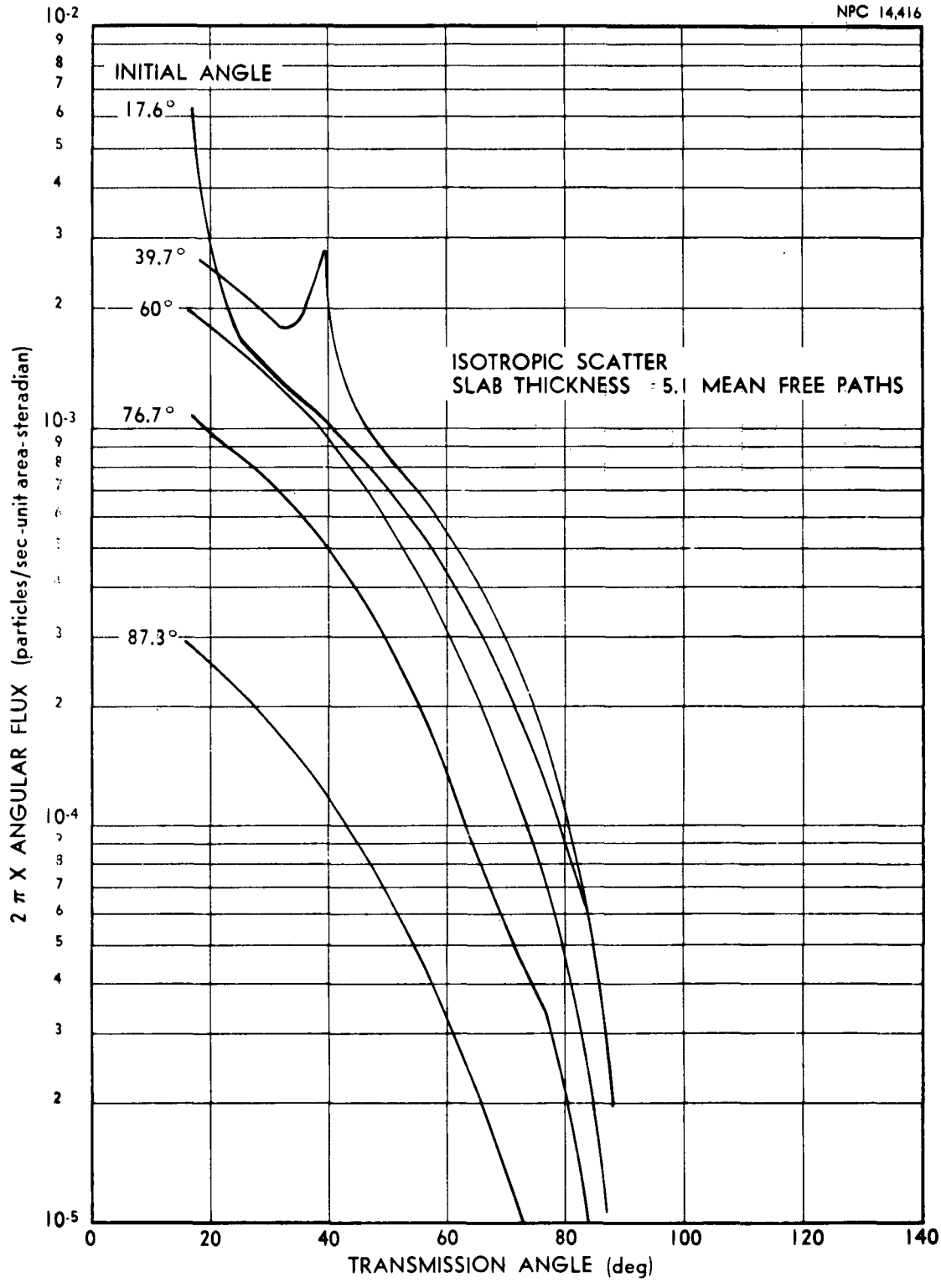

FIGURE 7. TRANSMITTED ANGULAR FLUX AS A FUNCTION OF TRANSMISSION ANGLE: ABSORPTION PROBABILITY = 0.5

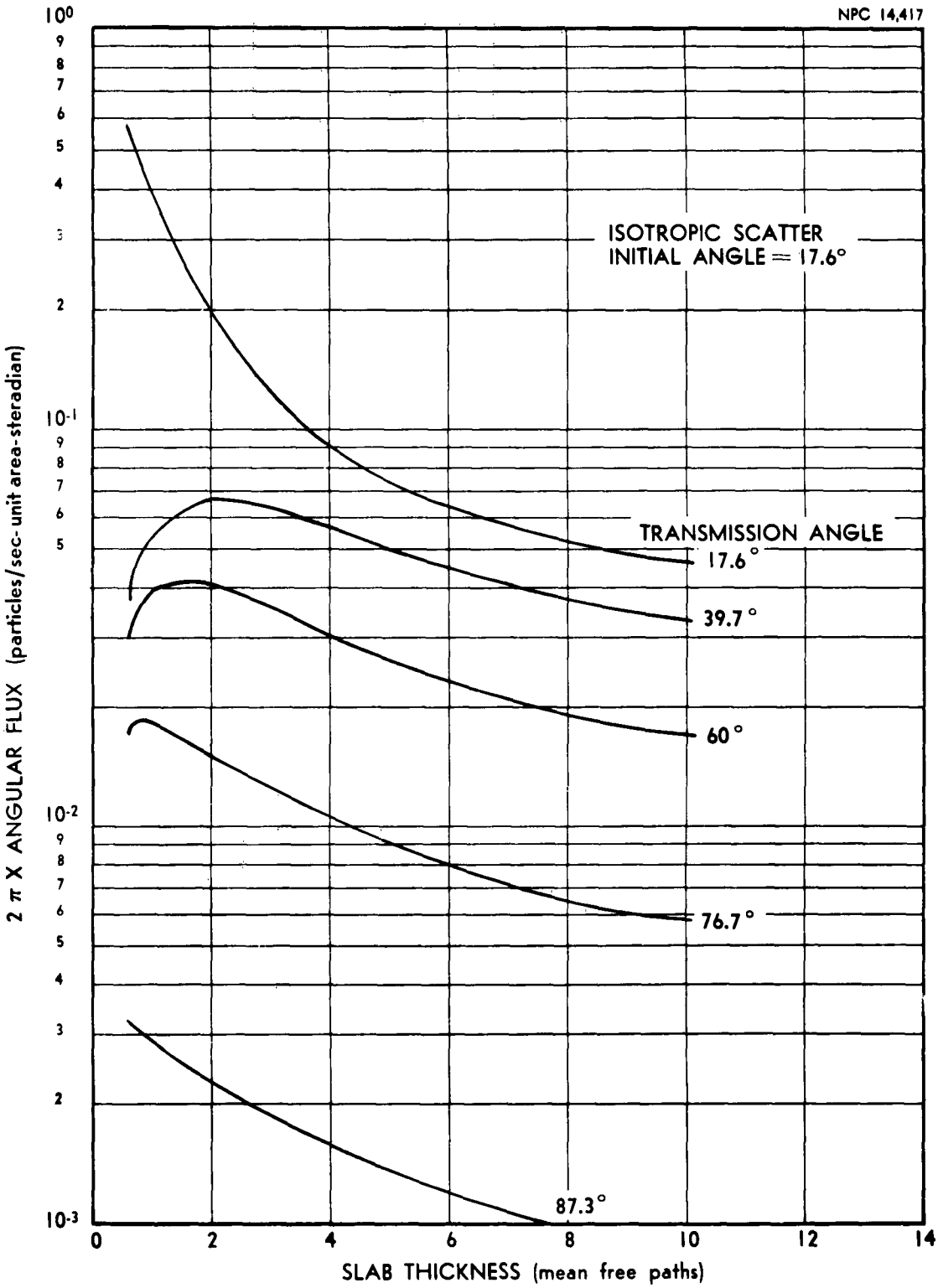

FIGURE 8. TRANSMITTED ANGULAR FLUX AS A FUNCTION OF SLAB THICKNESS: ABSORPTION PROBABILITY = 0.01

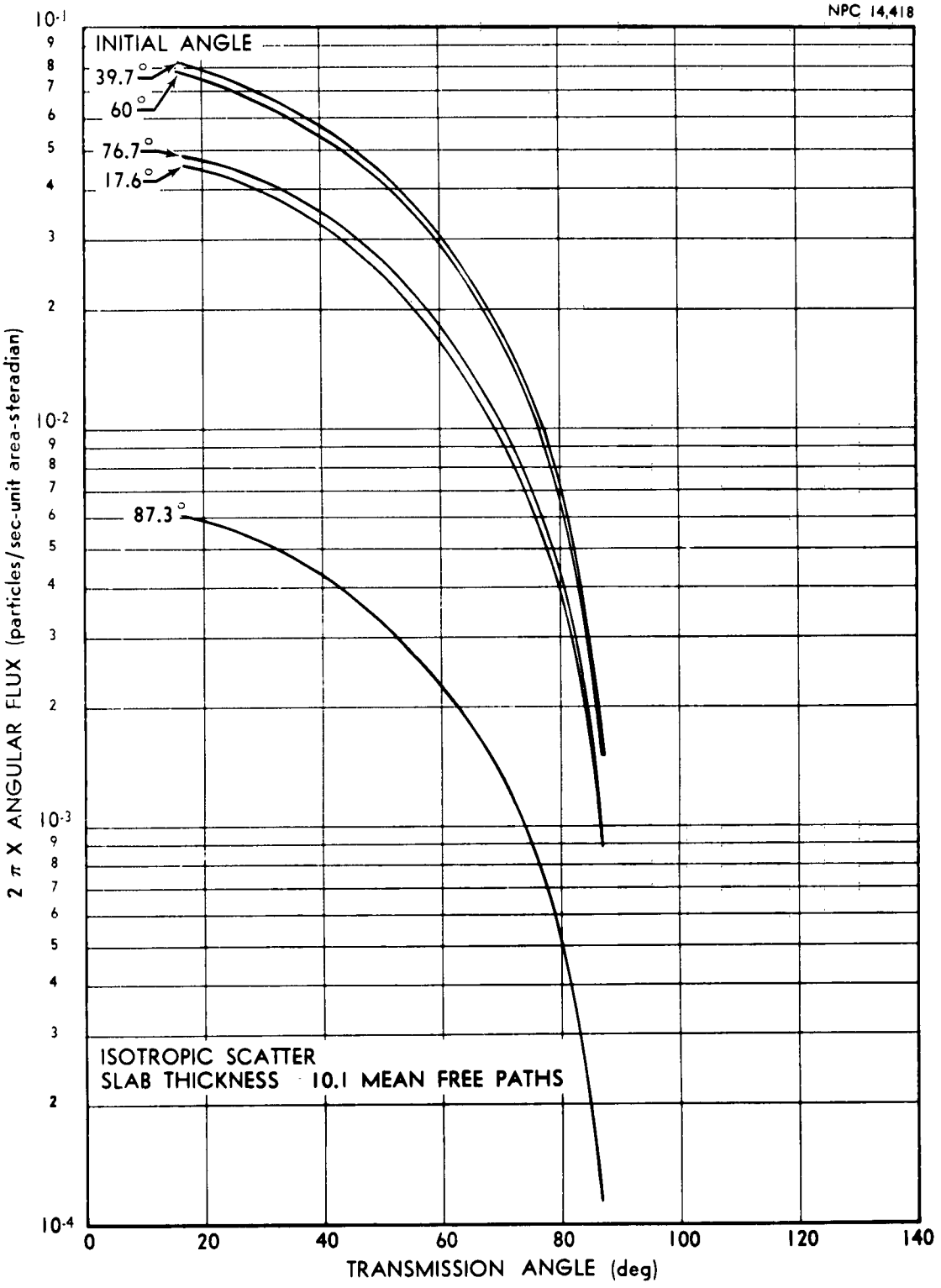

FIGURE 9. TRANSMITTED ANGULAR FLUX AS A FUNCTION OF TRANSMISSION ANGLE: ABSORPTION PROBABILITY = 0.01

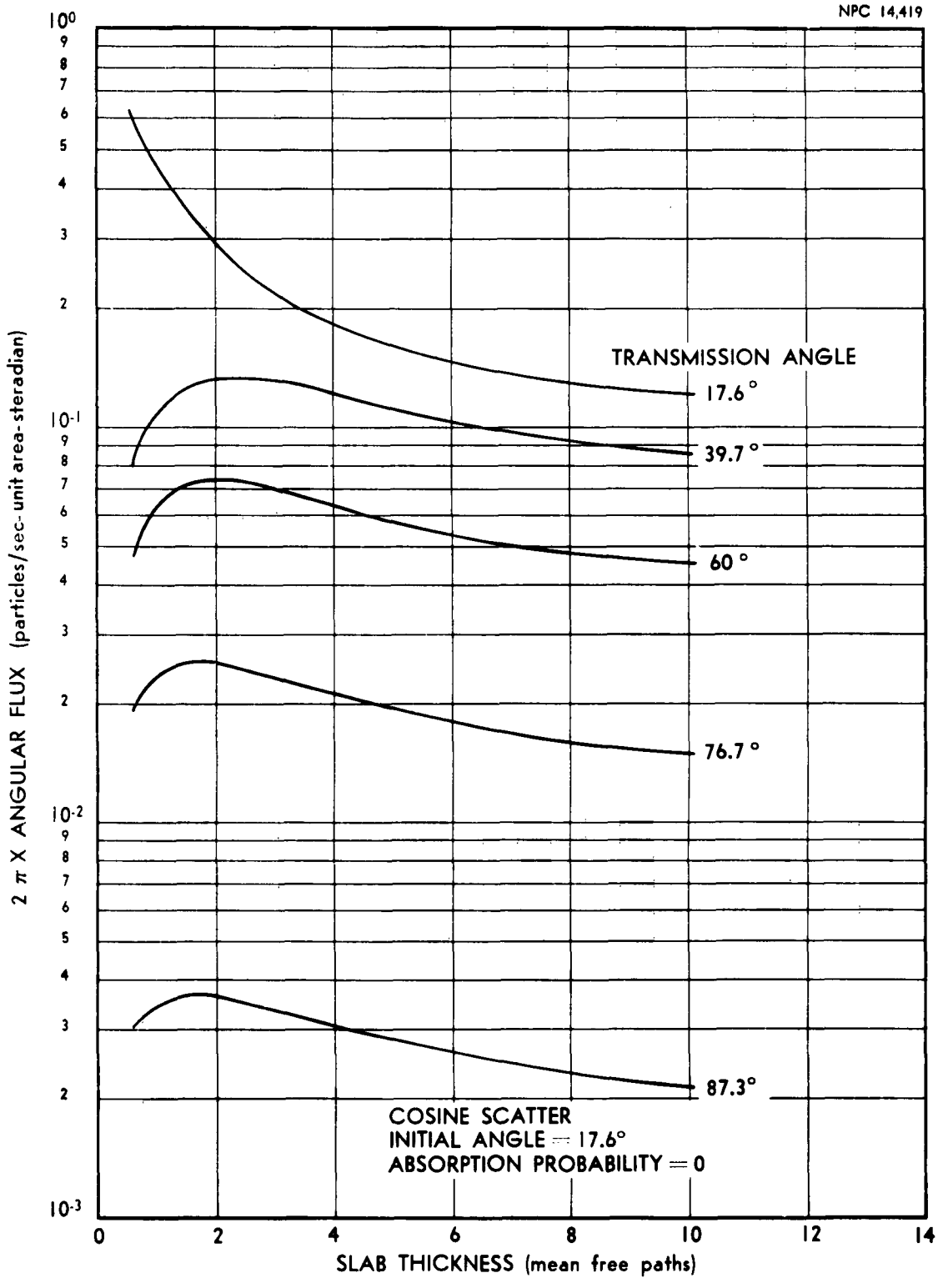

FIGURE 10. TRANSMITTED ANGULAR FLUX AS A FUNCTION OF SLAB THICKNESS: ANISOTROPIC SCATTER

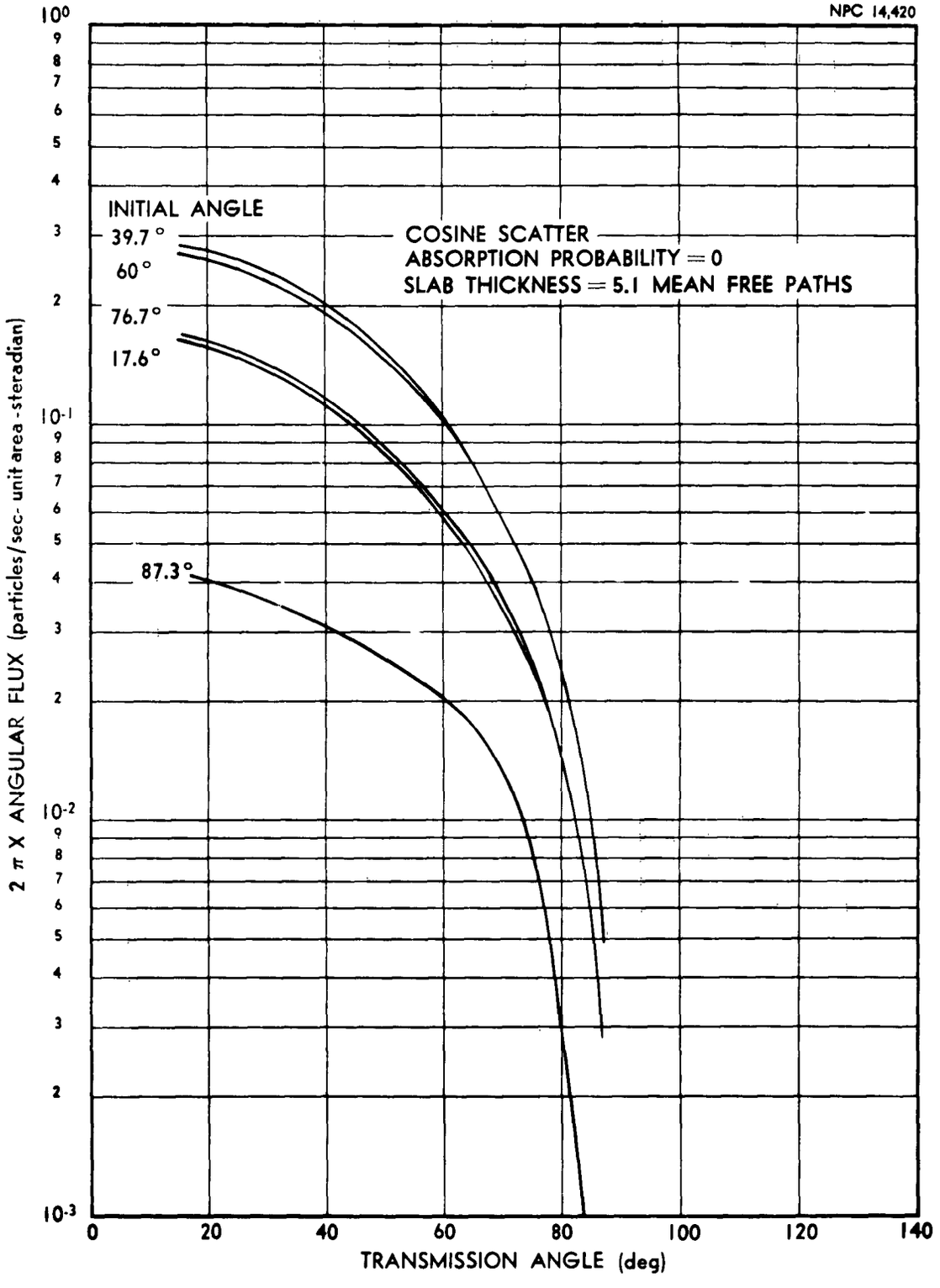

FIGURE 11. TRANSMITTED ANGULAR FLUX AS A FUNCTION OF TRANSMISSION ANGLE: ANISOTROPIC SCATTER

where the λ_r are the N eigenvalues of the N x N matrix C and the z_r are the matrices

$$z_r = \frac{\prod_s (\lambda_s U - C)}{\prod_s (\lambda_s - \lambda_r)}, \qquad r \neq s,$$

where U is the identity matrix. From physical considerations, it is seen that the eigenvalues, λ_r, are negative ($T(x) \longrightarrow 0$ as $x \longrightarrow \infty$). Also, there is at least one λ_m such that $|\lambda_m| \leq |\lambda_r|$ for all $r \neq m$. Thus, for x large enough, the mth term dominates and

$$T(x) \sim e^{\lambda_m x} z_m ,$$

which is of the form indicated by the numerical results of this section. That is, for x large enough, T(x) decays with the relaxation length $1/|\lambda_m|$ and the shape of the angular distribution is given by z_m. Thus, from a knowledge of the eigenvalues of C, one can determine the asymptotic transmitted angular flux. The accuracy of such an approximation depends, of course, on the accuracy of the thick-slab approximation and the equilibrium assumption and is, therefore, dependent on the shield material and slab thickness.

The fact that the numerical results were in accord with the trends predicted from collision-density considerations indicates that this approach may be useful in further studies of angular

distributions. For convenience, the conclusions based on such considerations and verified by the numerical results are listed below.

Perturbation	Effect on Transmitted Angular Distribution	Effect on Reflected Angular Distribution
Increase absorption probabilities	More peaked	Flatter
Increase slab thickness	More peaked	More peaked
Increase incident angle	Little change for thick slab	Flatter
Increase forward-scatter probability	Little change for thick slab - weak absorber	More peaked for small incident angle; flatter for grazing incidence

V. CONCLUSIONS

Although these initial studies indicate that definite advantages may be gained from the use of imbedding techniques in shielding problems, it should be noted that regardless of the method used the adequate description of energy and angular distributions requires the handling of large amounts of data and involves a considerable number of computations. Those familiar with the limitations of present computers have probably wondered how enough information may be carried in the machine to solve even the slab problem for combined neutron-gamma transmission. This may not be possible at present. Certainly the combination of neutron, gamma, and neutron-induced gamma penetration calculations with the optimization procedure into one program is not feasible. However, the author believes that the theoretical formulation of a unified approach to the shielding problem is needed - regardless of its immediate practical significance. Numerical experiments with simplified models, such as the one described in Section IV, may uncover new problems or shed some light on old ones - they may even result in the discovery of new shielding principles which are obscured by our present piece-meal view of the problem and our attempts to be realistic. Of more immediate importance, perhaps, is the possibility that the imbedding formulation of the shielding problem will suggest new approximations, such as those presented in Section III.

Thus, the imbedding method offers not only another mathematical approach to conventional shielding problems but also the possibility of the development of new physical approximations and, ultimately, the theoretical formulation of the shielding problem as a whole.

REFERENCES*

1. Ambarzumian, V. A., "Diffuse Reflection of Light by a Foggy Medium," Comptes Rendus (Doklady) de l'Academie des Sciences de l'URSS 38 (1943), 229-232.

2. Chandrasekhar, S., Radiative Transfer. Oxford: Clarendon Press (1950).

3. Bellman, R., Kalaba, R., and Wing, G. M., "Invariant Imbedding and Mathematical Physics I, Particle Processes," Journal of Mathematical Physics 1 (1960), 280-308.

4. Collatz, L., The Numerical Treatment of Differential Equations. Berlin: Springer Verlag (1960).

5. Bellman, R., Kalaba, R., and Prestrud, M., Invariant Imbedding and Radiative Transfer-I: Computational Results for Plane Parallel Slabs of Finite Thickness. The Rand Corporation (report to be published).

6. Bellman, R., Kalaba, R., and Prestrud, M., On a New Computational Solution of Time Dependent Transport Processes-I: One-Dimensional Case, The Rand Corporation Report P-2268 (30 March 1961).

7. Wing, G. M., "Invariant-Imbedding and Transport Theory - A Unified Approach," (to appear in the Journal of Mathematical Analysis and Applications).

8. Sheffield, R. D., Shield System Optimization - Gradient Non-Linear Programming. Convair-Fort Worth Report MR-N-186 (NARF-57-62T, December 1957).

9. Edmonson, N., Henrick, J. J., and Moss, T. A., Application of the Carlson S_n-Method to Calculation of Neutron Angular and Total Flux Distributions in a Spherically Symmetric Shield. Convair-Fort Worth Report MR-N-253 (NARF-60-11T, May 1960).

*All GD/FW reports published prior to July 1961 were referenced as Convair-Fort Worth Reports.

INITIAL DISTRIBUTION

MR-N-287
9 March 1962

Recipient	Copies
ASRCNL	2
ASRCPR-2	2
ASRMCE-1	2
ASRMPE-2	2
ASBMPT	2
ASTE	2
ASAPR	3
ASNPRI	2
GD/Convair	1
Convair-ASTRO	1
TIS	20
Lockheed-Ga.	1
Boeing AFPR	1
Douglas, Dept A26	1
North American	1
Pratt and Whitney	1
ORNL	1
NDA	1
Naval Ord Lab	1
Battelle-REIC	1
Air Univ Lib	1
Radioplane	1
Republic Avia	1
Vought-Aero	1
AFSWC (Tech Inf)	1
NASA-MSFC	1
NASA-Wash.	1
AFSC-NPPO	1
AFRDC-AE	1
ASRSMX-2	1
ASRKMA	2
ASTIA	10
TRG	1
Sandia	1
Bureau of Ships	1
DOFL (Chief-230)	1
GD/Astro, Att. D. G. Abshier	1
Aerojet-General Nucleonics, Attn. Friedman	1

Nuclear Aerospace Research Facility, General Dynamics/Fort Worth, Fort Worth, Texas.
THE APPLICATION OF INVARIANT IMBEDDING TO SHIELDING PROBLEMS, by R. E. Beissner. 9 March 1962. 71 p. incl. illus., 9 refs. (ER-N-267; NARF-61-41T)
(Contract AF33(657)-7201) Unclassified report

The fundamental concepts of the theory of invariant imbedding as applied to particle transport processes are reviewed and their applications to shielding problems are discussed. Two new approximate methods for predicting the transmission of particles through slabs of material are derived from the imbedding equations. One-velocity computations of the angular distributions of particles reflected and transmitted by slabs of varying thickness and composition are presented and analyzed.

UNCLASSIFIED

1. Neutrons and Gamma Rays
   - Shielding
   - Transmission
   - Reflection
   - Mathematical Analysis
I. Beissner, R. E.
II. Aeronautical Systems Division, Air Force Systems Command
III. Contract AF 33(657)-7201

UNCLASSIFIED

Nuclear Aerospace Research Facility, General Dynamics/Fort Worth, Fort Worth, Texas.
THE APPLICATION OF INVARIANT IMBEDDING TO SHIELDING PROBLEMS, by R. E. Beissner. 9 March 1962. 71 p. incl. illus., 9 refs. (ER-N-267; NARF-61-41T)
(Contract AF33(657)-7201) Unclassified report

The fundamental concepts of the theory of invariant imbedding as applied to particle transport processes are reviewed and their applications to shielding problems are discussed. Two new approximate methods for predicting the transmission of particles through slabs of material are derived from the imbedding equations. One-velocity computations of the angular distributions of particles reflected and transmitted by slabs of varying thickness and composition are presented and analyzed.

UNCLASSIFIED

1. Neutrons and Gamma Rays
   - Shielding
   - Transmission
   - Reflection
   - Mathematical Analysis
I. Beissner, R. E.
II. Aeronautical Systems Division, Air Force Systems Command
III. Contract AF 33(657)-7201

UNCLASSIFIED

Nuclear Aerospace Research Facility, General Dynamics/Fort Worth, Fort Worth, Texas.
THE APPLICATION OF INVARIANT IMBEDDING TO SHIELDING PROBLEMS, by R. E. Beissner. 9 March 1962. 71 p. incl. illus., 9 refs. (ER-N-267; NARF-61-41T)
(Contract AF33(657)-7201) Unclassified report

The fundamental concepts of the theory of invariant imbedding as applied to particle transport processes are reviewed and their applications to shielding problems are discussed. Two new approximate methods for predicting the transmission of particles through slabs of material are derived from the imbedding equations. One-velocity computations of the angular distributions of particles reflected and transmitted by slabs of varying thickness and composition are presented and analyzed.

UNCLASSIFIED

1. Neutrons and Gamma Rays
   - Shielding
   - Transmission
   - Reflection
   - Mathematical Analysis
I. Beissner, R. E.
II. Aeronautical Systems Division, Air Force Systems Command
III. Contract AF 33(657)-7201

UNCLASSIFIED